

# Materials Horizons

Accepted Manuscript

This article can be cited before page numbers have been issued, to do this please use: Z. Zhao, T. Wu, X. Li, Y. Chen and X. Meng, *Mater. Horiz.*, 2024, DOI: 10.1039/D4MH01180E.



This is an Accepted Manuscript, which has been through the Royal Society of Chemistry peer review process and has been accepted for publication.

Accepted Manuscripts are published online shortly after acceptance, before technical editing, formatting and proof reading. Using this free service, authors can make their results available to the community, in citable form, before we publish the edited article. We will replace this Accepted Manuscript with the edited and formatted Advance Article as soon as it is available.

You can find more information about Accepted Manuscripts in the [Information for Authors](#).

Please note that technical editing may introduce minor changes to the text and/or graphics, which may alter content. The journal's standard [Terms & Conditions](#) and the [Ethical guidelines](#) still apply. In no event shall the Royal Society of Chemistry be held responsible for any errors or omissions in this Accepted Manuscript or any consequences arising from the use of any information it contains.

## Wider Impact Statement

View Article Online  
DOI: 10.1039/D4MH01180E

Conventional catalysts preparation methods suffer from mild condition, prolong treatment and low energy transfer efficiency, thus leading to limited inherent nature of catalysts (such as: surface oxidation, agglomeration etc.). Recently, rapid Joule heating method, as novel synthesis method, has attracted widely attention due to the controllable kinetic conditions and eco-friendly operation, while the mechanisms, advantages and recent progress of such method has been concluded by few reviews. Herein, we systematically summarize basic fundamentals, fundamental parameters of Joule heating technique, as well as recent process in terms of effective modification strategies based on Joule heating. Meanwhile, the perspective suggestions and challenges for Joule heating methods on catalytic materials are put forward.

# **Progress and perspectives of rapid Joule heating for the preparation of highly efficient catalysts**

*Zhan Zhao, Ting Wu, Xiang Li, Yiming Chen and Xiangchao Meng\**

Key Laboratory of Marine Chemistry Theory and Technology (Ministry of Education), College of Chemistry & Chemical Engineering, Ocean University of China, Qingdao, Shandong, 266100, China.

*\*Corresponding author, E-mail: [mengxiangchao@ouc.edu.cn](mailto:mengxiangchao@ouc.edu.cn)*

9     **Abstract**

10     Functional catalytic materials play an important role in the field of environmental,  
11     biological, energy fields, etc., wherein the unique properties can be endowed by various  
12     synthesis strategies. However, the conventional catalysts preparation methods suffer  
13     from mild condition, prolong treatment and low energy transfer efficiency, thus leading  
14     to the situation of limited inherent characterisation of catalysts (such as: surface  
15     oxidation, agglomeration etc.). Recently, rapid Joule heating method, as a novel  
16     synthesis method, has attracted wide attention due to the controllable kinetic conditions  
17     and eco-friendly operation, while the mechanisms, advantages and recent progress of  
18     such method has been concluded by few reviews. Herein, we systematically summarize  
19     basic fundamentals, fundamental parameters of Joule heating technique, as well as  
20     recent processes in terms of effective modification strategies based on Joule heating.  
21     Meanwhile, the perspective suggestions and challenges for Joule heating methods on  
22     catalytic materials are put forward. This review provides understanding for designing  
23     advanced catalytic materials.

24     ***Keywords: catalysis; Joule heating; synthesis; functional nanomaterial; review***

25

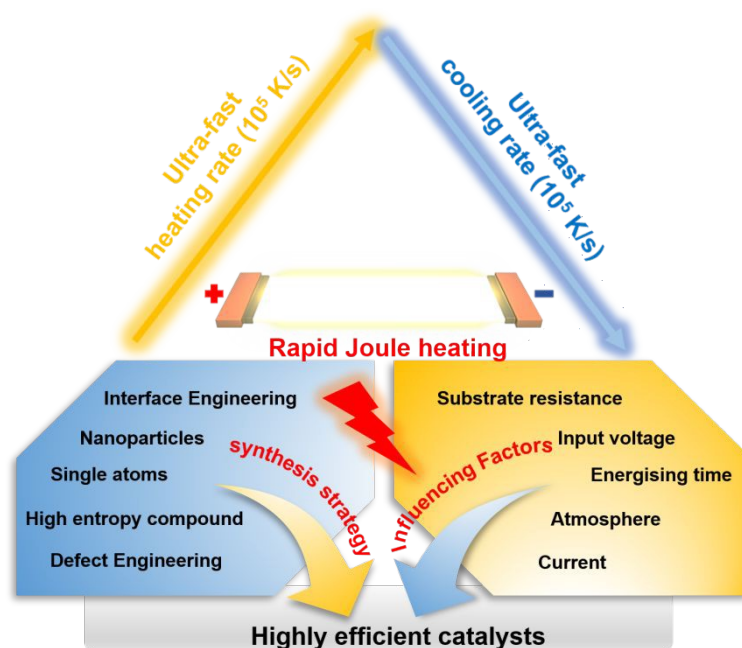
## 1. Introduction

Functional catalytic materials have showed great potentials in environmental, biological, energy fields, *etc.*<sup>1-5</sup>. Typically, by tailoring the compositions, morphologies, sizes of materials, the active sites for surface chemical reactions can be accordingly designed via suitable synthesis methods<sup>6</sup>. Recently, various nanomaterial preparation methods have been widely reported<sup>7-9</sup>, including solvothermal reaction<sup>9</sup>, electrodeposition<sup>10</sup>, ball milling, ultrasonic exfoliation and chemical disposition<sup>11-13</sup>. However, limited by the mild condition of the above methods, the precursor tends to be transferred to thermodynamically advantageous structure (such as: heterostructures and polycrystalline)<sup>14</sup>, wherein the inherent nature of materials is hindered. For instance, it is difficult to break through the immiscibility of elemental combinations to synthesize brand new single-phase multi-metallic materials. Meanwhile, the surface oxidation, agglomeration as well as weak interactions between different compositions can occur among most of the common synthesis processes, which leads to unsatisfactory catalytic performance<sup>15-17</sup>. Furthermore, it should be noted that most of the aforementioned methods are time-consuming<sup>18</sup> and limited by the large-scale manufacturing, thus leading to impoverished productivity of catalytic materials. Therefore, it is necessary and meaningful to find a series of facile and effective synthesis strategies, which can also provide harsh kinetic conditions to meet unique chemical and physical properties of catalytic materials.

46 Recently, Joule heating method has been considered to be an innovative and rapid  
47 synthesis of functional catalytic materials with the following advantages<sup>19-21</sup>: 1)  
48 Benefiting from the extremely fast heating rate (e.g.,  $10^5$  K/s)<sup>22</sup>, ultra-high temperatures  
49 among short period can be obtained, which is conducive to prevent active sites from  
50 further oxidation and agglomeration in long-term operation<sup>23</sup>. And the high-  
51 temperature treatment facilitates the transfer from metal salts/bulk metals to liquid alloy,  
52 which effectively realizes mutual solubility of multiple metals. 2) The following fast  
53 quenching provides sufficient dynamic conditions form metastable nanomaterials,  
54 which are characterized with structural distortion and defects, thus providing abundant  
55 uncoordinated catalytic sites<sup>24</sup>. 3) It should be noted that the short dwelling time (10-  
56 1000 ms) can effective synthesis and screen advanced catalysts, wherein the self-  
57 heating model with the precursors enables reduced energy consumption and facilitated  
58 production efficiency. 4) Materials can be effectively modified and the relevant reliable  
59 structure-effect relationships can be established via tuning the technical parameters of  
60 Joule-heating in catalyst synthesis<sup>25</sup>. Thus, the novel Joule heating method presents  
61 numerous advantageous features and provides a promising pathway to realize effective  
62 designing and synthesis of functional catalysts.

63 Herein, we systematically summarize recent processes for the catalytic materials  
64 synthesized via Joule heating as shown in Fig. 1. First, we introduce the basic  
65 fundamentals and fundamental parameters of Joule heating technique, including setup,  
66 mechanism for the ultra-fast heating/cooling as well as the characteristic advantage of

67 Joule heating. Then, based on the various functional catalytic materials, we review  
 68 effective modification strategies via Joule heating, which provide new understanding  
 69 for designing advanced catalytic materials. Finally, the perspective suggestions and  
 70 challenges for Joule heating methods on catalytic materials are put forward.



71  
 72 *Figure 1 Schematic illustration of rapid Joule heating method for synthesis highly efficient*  
 73 *catalysts.*

## 74 2. The rapid Joule heating technique

### 75 2.1 Mechanism of Joule heating

76 Joule heating is a novel rapid heating technique based on Joule's law that has recently  
 77 been employed in the synthesis of catalysts<sup>26</sup>, which is also known as ohmic heating.  
 78 Specifically, the generated voltage different on conductor can endow charge carriers  
 79 with kinetic energy, which collides with ions in the conductor, thus leading to an  
 80 amplification of atomic vibrations. This converts energy from the electric field into

81 thermal energy. In accordance with Joule's law, the heat generated by an electric current  
82 through a conductor is inversely proportional to the square of the current (Eq. 1).

83 
$$Q = I^2 R t \quad (1)$$

84 In the aforementioned equation,  $R$  represents the resistance of the substrate,  $I$  denotes  
85 the current flowing through the substrate,  $t$  signifies the energising time, and  $Q$  stands  
86 for the heat generated by the current flowing through the substrate.

87 In Joule heating technology, energy is fed into the system in the form of electrical  
88 energy. According to the law of conservation of energy, the input electrical energy can  
89 be divided into two parts (Eq. 2). One of these is ultimately converted into the form of  
90 heat and absorbed by the material, which is manifested as an increase in the temperature  
91 of the catalyst material. The other part is dissipated. The specific heat capacity and mass  
92 of the various materials can be related to the elevated temperature. This value is  
93 numerically equal to the part of the input electrical energy that is absorbed (Eq. 3).

94 
$$E_i = P t = E_a + E_d \quad (2)$$

95 
$$E_a = \xi \cdot E_i = c m (\Delta T) \quad (3)$$

96 In Eq. 2,  $E_i$ ,  $E_a$  and  $E_d$  represent the input, absorbed and dissipated electrical energy,  
97 respectively.  $P$  denotes the power, and  $t$  is the time of the continuous input of electrical  
98 energy.

99 In Eq. 3,  $\xi$  represents the absorption coefficient, which is primarily influenced by the  
100 material characteristics, reaction environment and heating method.  $c$  denotes the

Published on 06 November 2024. Downloaded on 11/7/2024 1:56:37 AM.

Materials Horizons Accepted Manuscript



specific heat capacity of the material,  $m$  is the mass of the material, and  $\Delta T$  is the temperature difference between the starting state and final state of the material.

$$\xi \cdot P / cm = \Delta T / t \quad (4)$$

Eq. 4 is derived from the aforementioned Eq. 2 and 3. From Eq. 4, suitable heated substrates should be selected to achieve the rapid temperature variation, wherein the factors of substrates, such as absorption coefficient, specific heat capacity and mass, should be considered. At present, the carbon-based materials with satisfactory thermal radiation coefficients as well as thermal conductivities are commonly used as substrates during the rapid Joule heating, which is characterized with the heating rate of  $10^3$ - $10^5$   $K \cdot s^{-1}$ . Meanwhile, in addition to the characteristics of the material, it can be observed that the heating rate  $\Delta T / t$  is also influenced by energy, time and space, and Table 1 summarizes the Joule heating setup parameters for the synthesis of catalysts.

Subsequent to the completion of the heating process, the supply of power is terminated, while the cooling process is initiated. The rate of cooling is primarily determined by the physical properties of the material and the manner in which the heat dissipation is achieved. The rate of heat dissipation can be expressed by Eq. 5, where  $\kappa$  and  $S$  represent the thermal conductivity and area of the material, respectively.

$$Q = \kappa \cdot S (\Delta T) \quad (5)$$

From Eq. 5, it can be seen that the increase of thermal conductivity can result in high thermal conductivity and fast cooling rate. In addition, the applied gas atmosphere, gas

flow rate and the condition with low temperature in the Joule heating process can significantly affect the cooling rate to obtain the materials with peculiar structure, which should also be rigorously controlled. For example, Hu *et al.* synthesized SF-Ru electrocatalyst with abundant stacking faults (35 and 196 mV @ 10 mA cm<sup>-2</sup> for hydrogen evolution reaction and oxygen evolution reaction, respectively), which was realized via rapid Joule heating and quenching under liquid nitrogen condition<sup>27</sup>. Compared with the *hcp*-Ru synthesized under Ar atmosphere, the SF-Ru was characterized with the tensile and compressive strain, which could affect the d-band center of Ru, thus adjusting the adsorbate binding.

**Table 1** Joule heating setup parameters for several materials

| Material                  | Voltage (V) | Current (A) | Temperature (°C) | Response time (s) | Recovery time (s) | Refs. |
|---------------------------|-------------|-------------|------------------|-------------------|-------------------|-------|
| Ag/C                      | -           | 20          | 500              | 0.5               | -                 | 28    |
| rGO aerogel               | 10          | -           | 2727             | 30                | -                 | 29    |
| Mo <sub>2</sub> C         | -           | -           | 1200             | 6                 | 1.5               | 30    |
| TMNs                      | 10          | 4           | 500              | 0.5               | -                 | 31    |
| CC-S                      | 80          | -           | 1227             | 0.3               | -                 | 32    |
| CMO/NF-x                  | -           | -           | 800              | 60                | -                 | 33    |
| DA-Ru <sub>NP+SA</sub> /C | -           | 20          | 950              | 1.5               | -                 | 34    |
| NiRu-CNTs                 | -           | -           | 1200             | 0.5               | -                 | 35    |
| Fe/TiO <sub>2</sub>       | 30          | 300         | 600              | 20                | -                 | 36    |
| PdSe <sub>2</sub> NPs/C   | -           | 12          | 480              | 60                | -                 | 37    |

## 2.2 Set up of Joule heating

Recently, two ultra-fast synthesis techniques have been investigated, which are based on the Joule heating effect: Flash Joule Heating (FJH) and Carbothermal Shock (CTS). Typically, the FJH technique relies on the capacitor bank that operates via high-voltage discharge. Meanwhile, the establishment of conductive pathways depends on the additives (such as graphene and carbon nanotube). While the heat generated from CTS technique is directly based on the carbon material, the carbon material and direct/alternating current are assembled to form a conductive pathway.

### 2.2.1 Set up of Flash Joule heating

Generally, the FJH setup consists of power supply, capacitor, flashing chamber, vacuum devices, diode electrical inductor and control systems for switching, as shown in Fig. 2a and b. Before the device is activated, the precursor is placed in a quartz or ceramic tube, wherein a certain proportion of conductive carbon material is added to obtain high conductive pathway. Meanwhile, the flashing chamber should be adjusted accordingly (such as gradual compressing) to increase the conductivity of system (1~1000  $\Omega$ ) as shown in Fig. 2c. Subsequently, the flashing chamber is located between the electrodes (brass screws), which is heated and driven by the discharge of the capacitor under specific gas atmosphere. The power source consists of a series of capacitors, which is characterized with ~0.2 F. Besides, the discharge time can be precisely controlled via a mechanical relay with millisecond delay. Finally, the precursor with carbon source can reach the target temperature (> 3000 K) in a very

short period of time (millisecond level). It should be noted that the temperature and duration of flash chamber can be controlled by setting the conductivity of additives and applied voltage of capacitor. The feedback of the temperature is realised via a temperature measuring system, wherein the real-time temperature is measured by fitting a blackbody radiation spectrum from 600 to 1100 nm as shown in Eq. 6. The  $\varepsilon_{gray}$  is the constant emissivity,  $T$  represents the measured temperature,  $h$ ,  $k_B$  and  $\gamma$  denotes the Planck constant, Boltzmann constant and fitting constant, respectively.  $\lambda$  and  $c$  are the physical quantities associated with light, which are the speed and wavelength of light, respectively.

$$B_{\lambda}(\lambda, T) = \gamma \varepsilon_{gray} \frac{2hc^2}{\lambda^5} \frac{1}{e^{hc/\lambda k_B T} - 1} \quad (5)$$

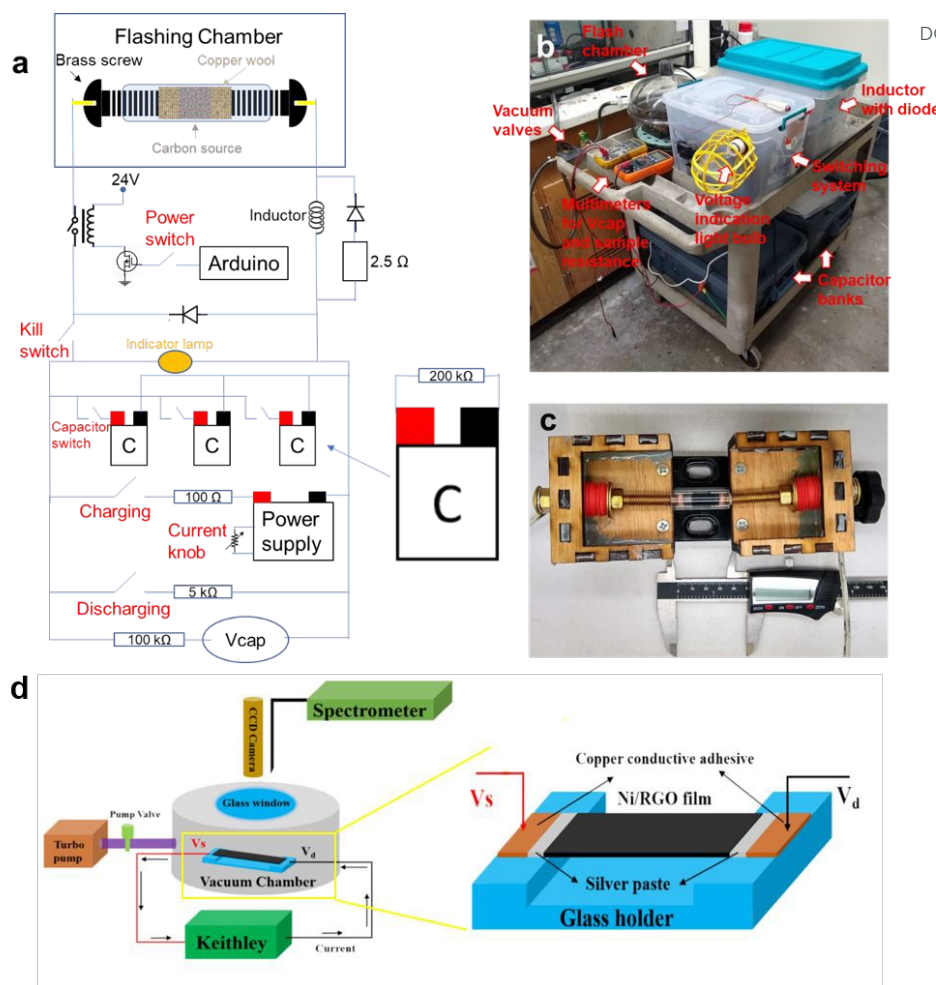


Figure 2 (a) The detailed schematic diagram of FJH setup. (b) Photo of the FJH setup. (c) Photo of the FJH reaction device. Reproduced with permission.<sup>38</sup> Copyright 2020, Nature. (d) The detailed schematic diagram of CTS setup. Reproduced with permission.<sup>39</sup> Copyright 2017, Wiley-VCH.

### 2.2.2 Set up of Carbothermal shock

The CTS setup includes electric power sources, conductive electrodes, a vacuum chamber, gas supply system, carbon-based substrate and a temperature sensor, wherein the CTS process utilises the heat generated by delivering a high electrical current to carbon-based substrate. For the operation of CTS device, two conductive electrodes are connected to two opposing ends of the substrate, and the DC power supply is connected

173 to the electrodes to form an electrical circuit. When the equipment is operated, the  
174 current flows through the electrodes to the substrate, which generates heat due to the  
175 resistance, thus leading to the instantaneous heating of the substrate. Consequently, the  
176 precursor material attached to the substrate can be in-situ transformed to the target  
177 material due to the instantaneous heating in the desired gas atmosphere. Meanwhile, in  
178 addition to the aforementioned instrumentation, the CTS setup includes a digital camera  
179 and a fibre-optic spectrometer, wherein the former is employed to capture images of  
180 the sample during the reaction process and the fibre-optic spectrometer is utilised to  
181 measure the temperature. Hu *et al.* reported the ultrafast CTS technique to convert  
182 micro-level Ni species to  $\sim 75$  nm Ni nanoparticles, which was realized on the rapid  
183 heating ( $\sim 2370$  K @ 0.06 s) on Ni@C/RGO<sup>39</sup>. It should be noted that the Nano  
184 Ni@C/RGO film was connected with copper wire by epoxy and silver colloid as shown  
185 in Fig. 2d. The obtained small Ni nanoparticles anchored on the RGO exhibited larger  
186 electroactive surface area, thus leading to excellent electro-oxidation activity for H<sub>2</sub>O<sub>2</sub>  
187 fuel ( $602 \text{ mA cm}^{-2}$  @ 0.2 V *vs.* Ag/AgCl). Compared with the complicated operation  
188 and the selection of various conductive additives of FJH, the CTS can utilise the carbon-  
189 based substrate synthesized by simple process, and is widely applied to synthesize  
190 functional alloy nanoparticles, entropic nanomaterials, nanocomposite materials.

## 2.3 Advantages for Joule heating technique

### 2.3.1 Transient feature

Currently, most of the conventional synthesis methods of materials are based on the thermochemical reactions, which are characterized with slowly continuous heating under near-equilibrium operating conditions. As a result, such methods suffer from low reaction rate, limited controllability and the waste of energy/reactants, especially for the in-situ synthesis of catalysts on the substrates, such as Ni foam, Cu foam and carbon paper<sup>40</sup>. Generally, the reaction rate based on the collisions of reactants can be adjusted by the high temperature and concentration of reactant, which is reflected by the classic nucleation and growth theories<sup>41</sup>, as shown in Eq. 6.

$$\frac{dN}{dt} = A \exp\left(-\frac{16\pi\gamma^3 v^2}{3k_B^3 T^3 (\ln S)^2}\right) \quad (6)$$

The  $N$  represents the number of nuclei,  $k_B$  denotes the Boltzmann constant.  $\gamma$  and  $v$  are the surface free energy and molar volume, respectively.  $A$  is associated with pre-exponential factor. The Joule heating makes it possible for the rapid nucleation of catalysts, which supplies the condition with high concentration and temperature reaction sites. Meanwhile, different from the traditional heating process, the Joule heating has been reported to realize the balance between high rate and controllability, and sensitive thermal modulation and periodic nucleation pulses via pre-set electrified process allows precisely synthesis of catalysts. Recently, Gao *et al.* reported an innovative wet-interfacial Joule heating method to effectively synthesize HKUST-1

211 with high crystallization rate ( $\sim 2 \mu\text{m s}^{-1}$ ), which was characterized with sub-second  
212 process and reactant-saving and was 6 orders of magnitude faster than traditional  
213 methods as shown in Fig. 3a<sup>40</sup>. The controllable nucleation and particle density could  
214 also be realized by the on-off pulses cycled of Joule heating.

215 Besides, the transient feature of Joule heating exhibits great potential in synthesizing  
216 the catalysts with specific morphology and structure, which minimizes the damage to  
217 substrate and functional component. For example, to avoid the damage to the  
218 transparent conducting oxide (TCO) substrate, Gao *et al.* synthesized metastable  
219 protohematite photoanodes for effective water oxidation via rapid Joule heating, which  
220 could obtain  $3.59 \text{ mA cm}^{-2}$  ( $1.23 \text{ V vs. RHE}$ )<sup>42</sup>. To solve the aggregation and oxidation  
221 of catalyst during the synthesis process, Meng *et al.* utilised rapid Joule heating method  
222 to provide ultra-high activation energy ( $> 1300 \text{ K}$ ) and synthesized highly active RuMo  
223 system, as shown in Fig. 3b. Specifically, the 3D morphology of RuMo catalyst could  
224 be remained compared with the catalyst prepared with the traditional temperature-  
225 programmed method, which played an important role in active area (Fig. 3c and d).  
226 Meanwhile, the rapid heating/cooling rate also endowed RuMo catalyst excellent  
227 surface wettability as shown in Fig. 3e.



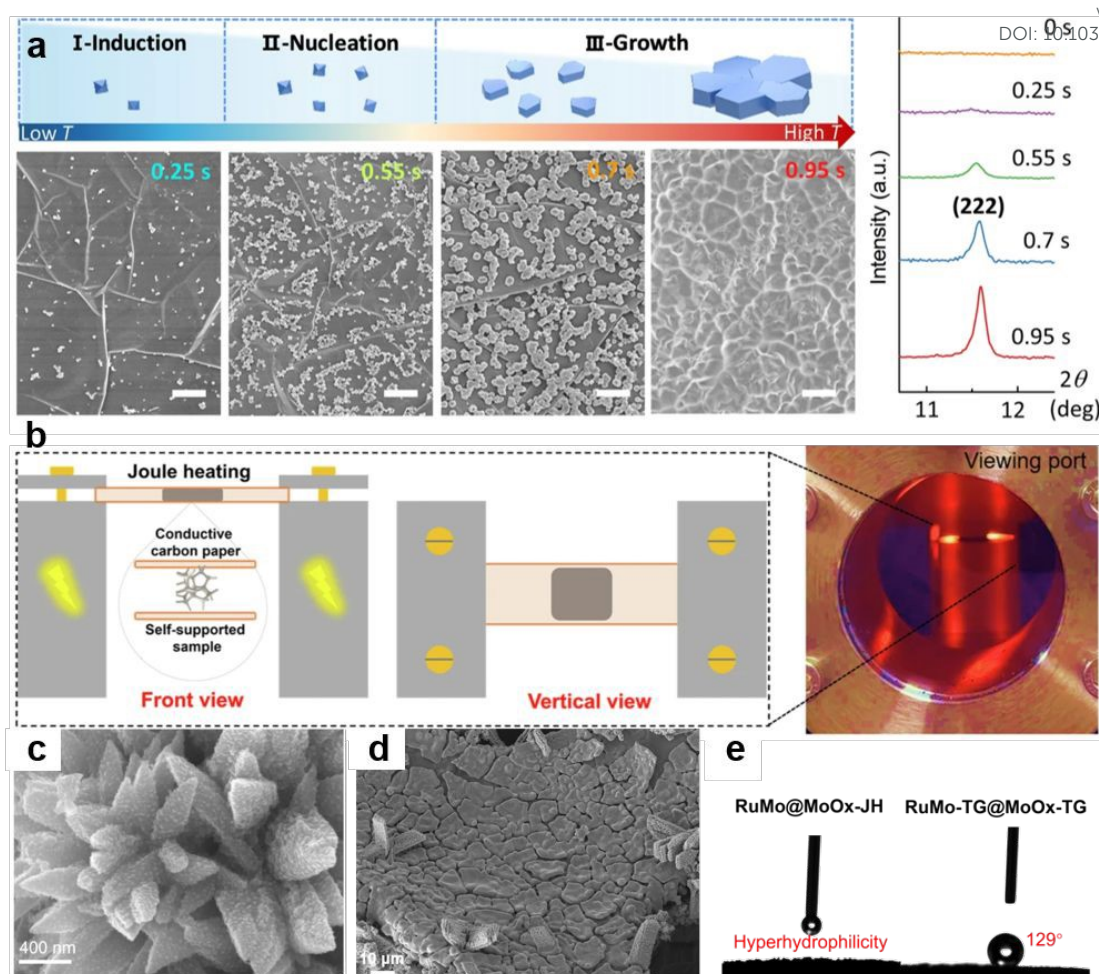


Figure 3 (a) The schematic diagram, SEM images and XRD patterns of structural evolution for HKUST-1. Reproduced with permission.<sup>40</sup> Copyright 2023, Springer Nature. (b) The schematic diagram and photo of the Joule heating setup. (c) SEM image of catalyst synthesized by Joule heating. (d) SEM image of catalyst synthesized by traditional method. Reproduced with permission.<sup>43</sup> Copyright 2024, Springer Nature.

### 2.3.2 Energy efficiency

Generally, the conventional heating methods, as indirect heating approach, involve the heating of resistive coil and transferring the heating to precursor, which is based on the radiation mechanism. However, the inferior power and heat dissipation limit the efficient use of energy. Conversely, the Joule heating, by mean of direct heating,

Published on 06 November 2024. Downloaded on 11/7/2024 1:56:37 AM.

Materials Horizons Accepted Manuscript

converts the energy of electricity to heating of sample, which is characterized with high heating efficiency and rapid temperature response. Meanwhile, such method can reduce the energy consumption due to the ultrashort reaction, wherein the Table 2 summarizes the reaction time and energy consumption of the Joule heating setup and conventional heating methods for the synthesis of catalysts. Recently, the effective synthesis of carbon nanomaterials from waste plastic via rapid Joule heating has been reported, wherein this synthesis strategy not only converts low-value waste plastics into high-value carbon nanomaterials, but also demonstrates high environmental friendliness and sustainability, with an 86-92% reduction in energy consumption and 92-94% reduction in global warming potential compared to conventional methods<sup>44</sup>. Therefore, the rapid Joule heating possess great potential for the effective synthesis of catalysts with eco-friendliness. Besides, it should be noted that the Joule heating has also been reported to be applied in the industrial thermochemical reactions that might suffer from the heat transfer processes and reaction equilibrium<sup>45</sup>. The temperature difference between the reactants/products and heater tube wall Heat transfer limitations can be avoided by placing the heating element, where the Joule effect occurs, directly in the reaction zone. Thus, the generated low temperature gradient minimizes by-product generation.

**Table 2** Synthetic process parameters for several materials

| Material                            | Synthesis method | Reaction time | Energy consumption  | Conventional synthesis method | Reaction time | Energy consumption   | Refs. |
|-------------------------------------|------------------|---------------|---------------------|-------------------------------|---------------|----------------------|-------|
| MoNi <sub>4</sub> /MoO <sub>x</sub> | Joule Heating    | 60 s          | 7 W h <sup>-1</sup> | Tube Furnace Calcination      | 2 h           | 6 KW h <sup>-1</sup> | 17    |

|  |                               |        |  |  |        |   |    |
|--|-------------------------------|--------|--|--|--------|---|----|
| NiFe alloy/MoO <sub>2</sub>  | Joule Heating                 | 180 s  | 21 W h <sup>-1</sup>                       | Tube Furnace Calcination               | 6 h    | 2 KW h <sup>-1</sup>  | 16 |
| Mo-Ru/CNTs   | carbotherm al shocking        | 40 s   | -  | Tube Furnace Calcination               | 2 h    | -   | 46 |
| RuMo@MoOx-JH   | Joule Heating                 | 60 s   | 7 W h <sup>-1</sup>                        | Tube Furnace Calcination               | 11.5 h | 17.2 KW h <sup>-1</sup>   | 43 |
| Ce-Co/CoO@CNTs   | Joule Heating                 | -      | -  | Tube Furnace Calcination               | 2 h    | -   | 47 |
| Co <sub>2</sub> Mo <sub>3</sub> O <sub>8</sub> /MoO <sub>2</sub> /NF | Joule Heating                 | 130 s  | -  | Tube Furnace Calcination               | 2 h    | -   | 15 |
| HS-NFS   | Thermal shock                 | 100 s  | -  | Tube Furnace Calcination               | 18 h   | -   | 48 |
| Pd <sub>3</sub> pb   | Joule Heating                 | 60 s   | -  | Traditional annealing                  | 3 h    | -   | 49 |
| Inorganic SEI  | Fast Heating                  | 150 ms | -  | Hydrometallurgical regeneration        | -      | About five times higher than Fast Heating                             | 50 |
| HKUST-1  | Wet-interfacial Joule heating | 0.25 s | $9.55 \times 10^{-6}$ kWh cm <sup>-2</sup> | Bulk-heating-based methods             | -      | About 10 <sup>6</sup> times higher than Wet-interfacial Joule heating | 40 |
| Graphite Anodes  | Flash recycling process       | ~1 s   | 10.6 kJ g <sup>-1</sup>                    | High-temperature-calcination method    | 2 h    | -   | 51 |
| N-CNTs   | Flash Joule heating           | 1 s    | -  | Tube furnace pyrolysis                 | 2 h    | -   | 52 |
| Asphaltene-derived flash graphene                                    | Flash Joule heating           | 100 ms | 20.55 kJ/g                                 | Conventional chemical vapor deposition | -      | -   | 53 |

|               |                     |       |                       |                                |   |                      |    |
|---------------|---------------------|-------|-----------------------|--------------------------------|---|----------------------|----|
| Ru-Fe@CF      | Joule heating       | 1 s   | -                     | Traditional calcination method | 3 h   | -                    | 54 |
| Spinel oxides | Joule heating       | 15 s  | 10 <sup>-1</sup> Wh/g | Hydrothermal                   | hours   | 10 <sup>3</sup> Wh/g | 55 |
| F-Si@rGO      | Flash Joule heating | 120 s | -                     | Tube furnace pyrolysis         | About 12000 times slower than Flash Joule heating | -                    | 56 |

257    2.4 Materials fabricated by Joule heating

258    The Joule heating process consists of several steps. The first step is to attach the  
259    precursor to the substrate. Next, a vacuum is applied to create the required gas  
260    atmosphere (air, Ar, N<sub>2</sub> or H<sub>2</sub>/Ar). Meanwhile, voltage and energization time are set  
261    and current is passed through the substrate, wherein the collision occurs between the  
262    precursor electrons and the substrate molecules, thus converting electrical energy into  
263    thermal energy. The temperature of the precursor rises rapidly, resulting in the mixing  
264    of metal atoms, nucleation and crystal growth. The following sections systematically  
265    introduce the progress of Joule heating in synthesizing different materials.

266    2.4.1 Carbon-based materials

267    Currently, the carbon-based materials, as potential catalyst, have attracted wide  
268    attention in industrial production, which exhibit exceptional light absorbing properties,  
269    excellent conductivity and physical stability<sup>57</sup>. Meanwhile, the abundant resources, eco-

270 friendliness, no toxicity and low cost-effectiveness endow carbon-based materials with  
271 the potential for large-scale generation. Consequently, carbon-based catalysts possess  
272 great implementation prospects in plentiful fields, such as energy storage devices,  
273 electrocatalysis, photocatalysis, photodetectors<sup>58</sup>. Generally, several common methods  
274 have been applied to synthesized carbon-based materials, such as Scotch tape method,  
275 chemical vapor deposition, redox reaction and liquid-phase exfoliation<sup>59</sup>. However, the  
276 effective synthesis is limited in terms of preparation of large-sized samples, precise  
277 design for morphology, product quality and large-scale preparation. The Joule heating,  
278 as an innovative method with rapid reaction speed and controllability, can serve as ideal  
279 technique for effective synthesize the carbon-based materials. Typically, the extremely  
280 fast heating rate (e.g.,  $10^5$  K/s) generated by Joule heating can rebuild conjugated  
281 backbone in defective graphene blocks, which exhibits satisfactory conductivity as well  
282 as carrier mobility of carbon films<sup>60</sup>. For example, Gao *et al.* proposed a roll-to-roll  
283 process based on Joule heating<sup>61</sup>, which was capable of continuously producing large-  
284 area, high-quality graphene films (electrical conductivity:  $4.2 \times 10^5$  S/m, thermal  
285 conductivity:  $1285 \pm 20$  W/mK) as shown in Fig. 4a. It should be noted that heating to  
286 high temperatures ( $\sim 2400$  °C) at constant voltage can further remove structural defects  
287 and impurities. The roll-to-roll Joule heating method offers significant advantages in  
288 terms of preparation time and energy consumption over the conventional electric  
289 furnace heating methods, wherein the Joule heating consumed less than 3 KW electrical  
290 power. James *et al.* synthesized one-dimensional (1D) and 1D/2D hybrid carbon

nanomaterials form plastic waste using Flash Joule Heating (FJH) technology (Fig. 4b), which was characterized with fast reaction, scalable synthesis and avoided the use of solvents or water, thus outperforming conventional chemical vapour deposition as shown in Fig. 4c<sup>44</sup>. Meanwhile, it has been shown that by adjusting the reaction conditions of FJH (e.g. voltage, capacitance, catalyst type and concentration, etc.), the morphology and size of the synthesized carbon nanomaterials can be effectively controlled, including different structures such as nanotubes, nano-fibres and nanoribbons. The rapid heating and cooling process generated by Joule heating provides a simple and rapid method of uniformly loading metal nanoparticles onto carbon carriers, allowing precise tuning of the size, structure and dispersion of the active sites such as alloy nanoparticles, single-atom. For instance, Wang *et al.* realized ultrafine active NiRu alloy nanoparticles (NiRu-CNTs) dispersed on nitrogen-doped carbon nanotubes (N-rich CNTs) by Joule heating as shown in Fig. 4d, which was served as effective electrocatalyst for hydrogen evolution reaction (5.1 mV@10 mA cm<sup>-2</sup>)<sup>62</sup>. The research not only demonstrated that the Joule heating technique is an effective strategy for the preparation of ultrafine-sized and well-dispersed alloys on carbon-based substrate, but also provided an important reference for the design and development of new high-efficiency and low-cost electrocatalysts.



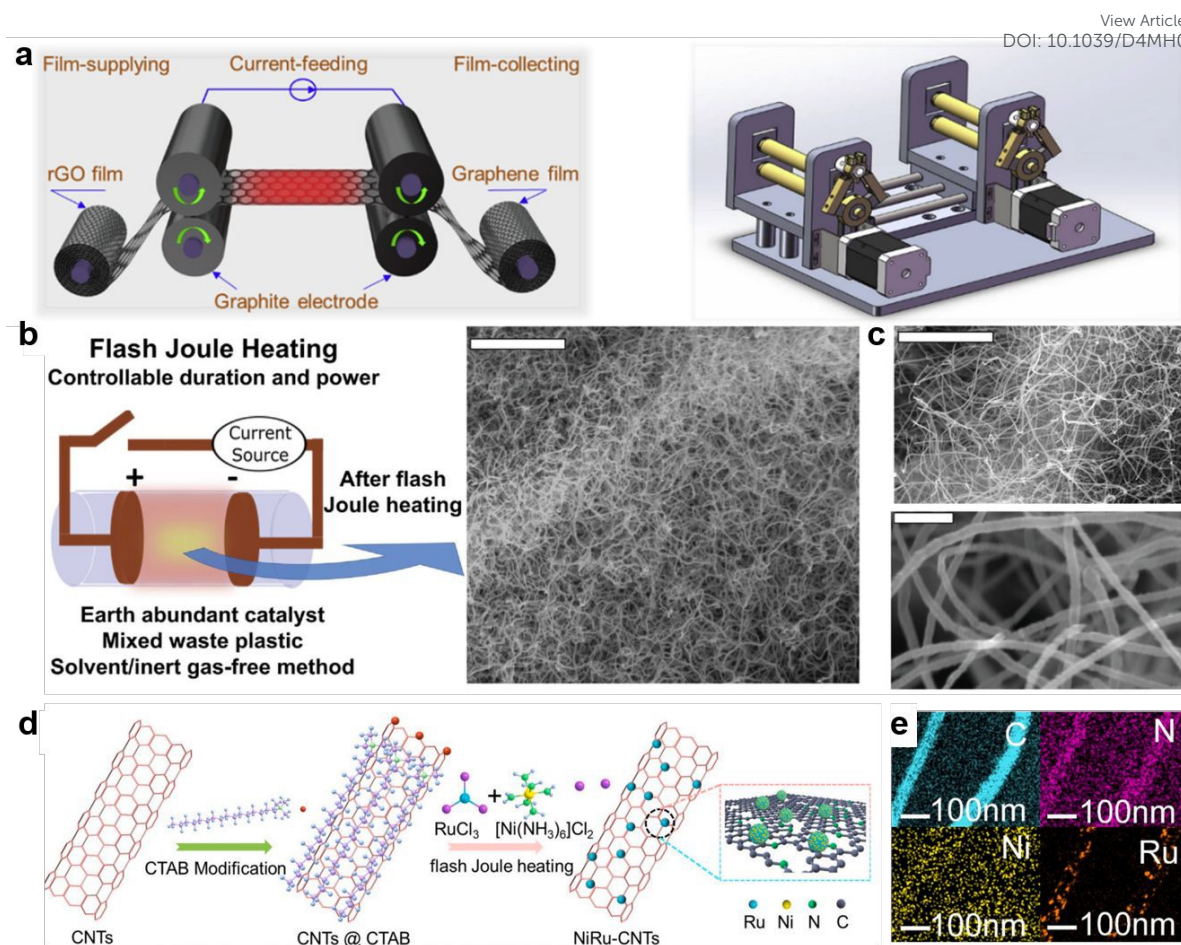


Figure 4 (a) The schematic diagram of roll-to-roll process based on Joule heating.

Reproduced with permission. <sup>61</sup> Copyright 2019, Elsevier. (b) The schematic diagram of the

FJH setup with the (c) SEM image of nanomaterials. Reproduced with permission. <sup>44</sup>

Copyright 2023, Wiley-VCH. (d) The schematic diagram of sample synthesis process. (e)

EDX elemental mapping images of sample. Reproduced with permission. <sup>62</sup> Copyright 2023,

Elsevier.

#### 2.4.2 Metal-based materials

The metallic materials have been considered as essential components in industrial catalytic production due to the excellent electrical and thermal conductivity, associated with high hardness and strength, which can also be applied as effective catalysts with abundant active sites and high intrinsic activity <sup>63</sup>. However, the conventional methods

321 for synthesising metallic materials such as intermetallic compounds typically rely on  
322 prolonged annealing treatments, which tend to sinter and aggregate the metallic  
323 particles, thus degrading the catalytic properties. Consequently, synthesising the  
324 metallic catalysts with highly ordered and uniform distribution on the substrate in a  
325 short time has been considered as a challenge in the field of materials science. Recently,  
326 the rapid Joule heating method with ultra-fast high-temperature sintering is recognized  
327 as an effective technique, which is particularly beneficial to the application with large-  
328 scale production of material and effectively avoids the thermodynamically driven  
329 aggregation and oxidation of metal active sites<sup>43</sup>. Meanwhile, the rapid Joule heating  
330 method also allows materials to be produced with high densities, which is important for  
331 specific applications such as solid-state batteries. Hu *et al.* obtained ultrafine silver (Ag)  
332 nanoparticles on carbon nanofibers via a fast Joule heating method (~1600 K@20 ms),  
333 wherein the uniform Ag nanoparticles served as nano-seeds to guide the deposition of  
334 lithium to effectively address the problems of dendrite growth and interfacial instability  
335 on lithium metal battery anodes<sup>64</sup>. And the as-prepared Ag-based anode exhibited low  
336 overpotential (0.025 V) with long cycle life. Meanwhile, Zachariah *et al.* utilized Joule  
337 heating to synthesize uniformly distributed nanoparticles (Al, Pd, Si, Sn) in reduced  
338 graphene oxide (RGO) matrices, which could realize the melting and self-assembling  
339 micron-sized metal or semiconductor particles into nanoparticles in a short time (1700  
340 K@ 0.01 s)<sup>65</sup>. Benefiting from the barrier effect of the defects on RGO and rapid  
341 melting under Joule heating, the Al nanoparticles could avoid the merge and



342 agglomerate, which were driven by the surface energy. And the molecular dynamics  
343 (MD) simulations proved the generated defects and graphene boundaries provided  
344 barrier to limit the thermo-activated random walk of Al species, thus leading to the  
345 uniform distribution.

346 It should be noted that the Joule heating process can reach high temperature (up to  
347 3000 °C), which is appropriate for sintering various high melting point metals and  
348 obtaining wide range of metal and alloys. The non-equilibrium Joule heating-based  
349 approach can also effectively solve the problem of phase separation of high entropy  
350 nanoparticles/alloy due to the rapid heating/cooling rates, even in immiscible elemental  
351 combinations. Chen *et al.* ensured the well mixing and reaction of component to  
352 successfully synthesize high entropy metal selenides via Joule heating, which avoided  
353 the problem of temperature gradients that are common in conventional heating  
354 methods<sup>66</sup>. It should be noted that the HEMS exhibited a low overpotential of 222 mV  
355 to obtain the current density of 10 mA cm<sup>-2</sup> for OER and showed little degradation in a  
356 1000 h durability test. Theoretical investigations showed that the asymmetric Cu-Co-  
357 Ni active unit played an important role in improving the activity and durability by  
358 modulating the interplay of oxygen-containing intermediates. In addition, such  
359 synthesis process is capable of modifying the microstructure of the material to form a  
360 more homogeneous and stable nanostructure, thereby improving the catalytic properties  
361 of the material<sup>67</sup>. Xu *et al.* successfully synthesized PtFeCoNiMn high-entropy nano-  
362 alloy on nitrogen-doped carbon (PtFeCoNiMn/NC) as effective electrocatalysts for

oxygen reduction reaction (ORR) and oxygen evolution reaction (OER) via the ultra-fast Joule heating technique, wherein the strong thermal driving force of the Joule heating process promoted the formation of high-entropy alloy nanoparticles from the absorbed metal ions on NC<sup>68</sup>. Meanwhile, the rapid Joule heating plays an important role in enabling the formation of a strong bond between the alloy nanoparticle catalyst and the conductive substrate, which improves the long lifetime of the metal-based catalyst for catalysis and energy conversion. Recently, Yao *et al.* induced the high-entropy alloy to the defect sites of carbonised wood, wherein the carbon atoms could move to the surface of high-entropy alloy nanoparticles to form a carbon protective shell. This treatment significantly strengthened the interface between the high-entropy alloy nanoparticles and the activated carbon protective layer, which remained active (7 mV@10 mA cm<sup>-2</sup>) during 500 hours electrolysis<sup>69</sup>.

#### 2.4.3 Inorganic non-metal-based materials

The range of inorganic non-metal-based materials is wide, such as glass, ceramics, and cement etc, which consists of oxides, carbides, nitrides and silicon-based material. Among them, porous ceramic materials are widely applied in the fields such as electrodes, photopolarimetry and catalyst supports, which have also attracted much attention in the field of thermal insulation materials with the features of low thermal conductivity as well as excellent chemical inertness<sup>70</sup>. Recently, Chu *et al.* have successfully developed a 9-cation porous high-entropy diboride ceramic ((Hf<sub>1/9</sub>Zr<sub>1/9</sub>Ta<sub>1/9</sub>Nb<sub>1/9</sub>Ti<sub>1/9</sub>Cr<sub>1/9</sub>Mo<sub>1/9</sub>V<sub>1/9</sub>W<sub>1/9</sub>)B<sub>2</sub>) with a unique multi-scale structural

384 design via Joule heating<sup>71</sup>, wherein the such ceramic material not only exhibited  
385 excellent mechanical strength (337 MPa) at room temperature, but also good thermal  
386 insulation properties (thermal conductivity of 0.76 W/(m K)) as shown in Fig. 5a. In  
387 detail, under the borothermal reduction, the uniformly distributed submicron pores  
388 could be generated due to the production and release of the significant amount of B<sub>2</sub>O<sub>3</sub>  
389 gas. Meanwhile, the authors sintered the diboride ceramic with 10 seconds by using  
390 rapid Joule heating synthesis technology, wherein the generated strong connections  
391 between grains as well as interface between building blocks in the nanoscale played  
392 important roles in thermal insulation and mechanical properties.

393 Currently, the energy density of graphite as an anode material for lithium-ion batteries  
394 is close to its theoretical limit, and the inorganic non-metal-based materials (such as  
395 silicon-based material), with extremely high theoretical specific capacity and low  
396 delithium potential, have emerged as a promising candidate for improving the energy  
397 density of batteries<sup>72</sup>. However, the volume expansion of inorganic non-metal elements  
398 (such as silicon) during charging and discharging can lead to particle fragmentation and  
399 continued formation of SEI layers, which in turn degrades battery capacity degradation.  
400 Recently, strategy of encapsulating silicon nanoparticles in carbon matrices to improve  
401 stability and electrochemical performance via Joule heating has been reported. Tang *et al.*  
402 anchored silicon nanoparticles through the formation of silicide 'rivets' between  
403 silicon and graphene via FJH technique to avoid the phase separation and structural  
404 instability (Fig. 5b)<sup>56</sup>. After the electrochemical cycling, the F-Si@rGO synthesized via

FJH maintained the structural integrity due to the strong anchoring between the silicon and carbon matrix, while the S-Si@rGO synthesized with slow heating rate showed severe fragmentation of silicon particle and overgrowth of the SEI layer. Therefore, the homogeneous lithiation and interfacial stability of F-Si@rGO, endowed by rapid Joule heating, contributed to the reduction of microcrack formation during the long-term cycling process, thus maintaining the electrical conductivity of the electrode. Meanwhile, the feasibility of mass-producing of sample has been verified by integrating freeze-drying and FJH techniques as shown in Fig. 5c.

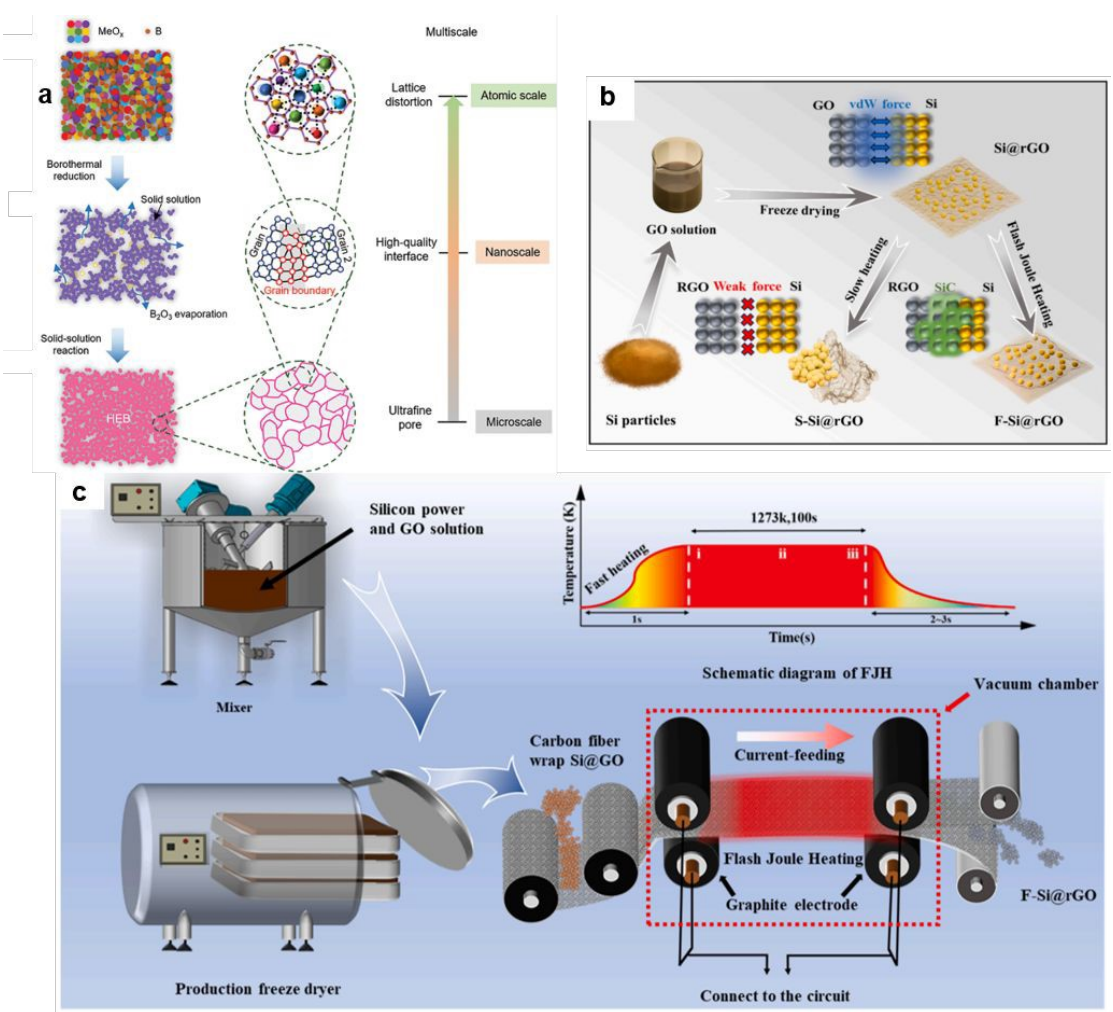


*Figure 5* (a) The schematic diagram of the fabrication of 9-cation porous high-entropy diboride ceramic. Reproduced with permission. <sup>71</sup> Copyright 2024, Wiley-VCH. (b) The schematic diagram of the fabrication of silicon-carbon matrix with (c) the schematic diagram of FJH setup for mass-producing of sample. Reproduced with permission. <sup>56</sup> Copyright 2024, Elsevier.

## 2.5 Characteristics of materials synthesized via Joule heating

### 2.5.1 Dispersibility

Heterogeneous catalysis plays a pivotal role in contemporary industrial processes, with the catalytic reaction predominantly occurring on the surface of solid catalysts<sup>73</sup>. In order to enhance the performance of catalysts, researchers have sought to increase the surface area to volume ratio, such as reducing the size of metallic/non-metallic particles while maintaining a high particle density on the surface<sup>74</sup>. However, the increased surface energy of metal atoms, during the preparation of catalysts at high temperature, gives rise to the tendency to aggregate and form bulky catalysts<sup>43</sup>. The conventional high-temperature pyrolysis methods, despite the widespread application for catalyst synthesis, are hindered for the industrial applicability due to the limitations in thermal diffusion, particle aggregation, and phase separation. Ultrafast Joule heating technology is capable of effectively circumventing metal atom aggregation and maintaining the stability of catalytic particle dispersion through rapid energy input and instantaneous quenching<sup>65</sup>. Tian *et al.* presented the versatile and efficient CTS method for the synthesis of ultra-small and high-density nanoparticles that are homogeneously dispersed and anchored on two-dimensional porous carbon<sup>75</sup>. Typically, in comparison

with conventional tube furnace annealing, the CTS has the advantage of reducing the time by at least five orders of magnitude, and shrinking the size from 27 nm to 1.9 nm with the increase of electrochemical surface area (ECSA) by a factor of 3.8. It should be noted that the rapid Joule heating provides a simple and efficient universal transient nanoparticle synthesis route.

### 2.5.2 Phase purity

The conventional methods of materials synthesis typically necessitate elevated temperatures in excess of 600°C and protracted reaction times spanning hours to days, which are predicated on equilibrium thermodynamics, thereby rendering it challenging to precise control over the phase structure and crystal morphology of the material<sup>76</sup>. In recent years, researches investigating the synthesis of highly ordered and well-dispersed intermetallic nanoparticles using the Joule heating technique have been conducted. For example, Hu *et al.* employed rapid Joule heating method to synthesise L12 ordered Pd<sub>3</sub>Pb nanoparticles with an average diameter of approximately 6 nm<sup>49</sup>, which was achieved by subjecting the reaction mixture to a heating period of 60 seconds at 1600 K. It should be noted that the degree of orderliness of the Pd<sub>3</sub>Pb structure could be evaluated by analysing the intensity of the superlattice XRD peaks (100) and (110), wherein the degree of ordering in Pd<sub>3</sub>Pb increased gradually with the duration of the heating period and reached complete ordering after 60 seconds. In the contract, the conventional annealing method (~1273 K@3 h) yielded Pd<sub>3</sub>Pb intermetallic nanoparticles with large average size of approximately 85 nm and a low ordering degree

457 of merely 60 %. Tour *et al.* designed novel Flash-within-flash synthesis technique to  
458 avoid the possible impurities in the product<sup>76</sup>, which might be caused by the conductive  
459 additives or substrates. In detail, The Flash-within-flash synthesis technique utilised  
460 two quartz vessels, wherein the external flash vessel contained a conductive feedstock  
461 such as metallurgical coke, while the internal semi-closed reactor contained the target  
462 reactants. Most importantly, the novel technique, based on Joule heating, not only  
463 enabled the gram-scale synthesis of target samples, but also realized the phase-selective  
464 and single-crystalline bulk powders, which effectively produced target samples with  
465 high purity.

466 Besides, the Joule heating, with high temperature (up to 3000 °C) and rapid heating rate,  
467 can also effectively deconstruct and recycle real-life waste materials such as polyolefin  
468 plastic waste and waste lithium-ion battery cathode to synthesize functional materials  
469 with high phase purity<sup>77</sup>, which shows high environmental and economic benefits. For  
470 example, Viachos *et al.* employed one-step Joule heating method to effectively convert  
471 polyolefin plastic waste to light olefins (C<sub>2</sub>-C<sub>4</sub>) with 90% product fraction<sup>78</sup>. It should  
472 be noted that the pulsed treatment coupled with steam co-feeding could facilitate highly  
473 efficient selective deconstruction, while simultaneously reducing catalyst deactivation.  
474 Tou *et al.* presented an innovative solvent- and water-free FJH technique for the  
475 efficient recovery of waste lithium-ion battery cathode materials<sup>77</sup>. Following the  
476 application of FJH treatment, the three-dimensional structure of the cathode material  
477 was observed to remain intact, and the presence of metallic impurities was effectively



eliminated through the use of magnetic separation techniques. Meanwhile, the concentration of Cu and Al was found to decrease significantly, thereby ensuring the enhanced purity of the re-synthesised cathode material.

### 2.5.3 Structure

The designed structure of functional catalysts, synthesized via Joule heating methods, plays an important role in determining the catalytic performance, which can optimize essential factors such as adsorption/desorption of reaction intermediates, ion migration and electron transport<sup>79</sup>. For example, Chen *et al.* prepared hetero-structured catalysts (W-W<sub>2</sub>C/G) using the FJH method, which resulted in the spontaneous generation of an internal electric field at the hetero-structured interface, driven by the difference in the work function of W (5.08 eV) and W<sub>2</sub>C (6.31 eV)<sup>80</sup>. Such phenomenon effectively accelerated the movement of electrons and ions in catalysts, thus facilitating the sulphur reduction reaction (SRR) process and effectively suppressing the polysulfide shuttling effect. Finally, benefiting from the construction of work function at interface via Joule heating, the W-W<sub>2</sub>C/G exhibited excellent performance (665 mAh g<sup>-1</sup> at 5.0 C). Cao *et al.* utilized the Joule heating with transient discharge to enhance the degree of graphitisation for as-prepared hollow carbon spheres, accompanied by improvement in the crystal structure and electrical conductivity of the materials<sup>81</sup>. The graphene-like hollow spheres (L-GHS), as anode materials for lithium-ion batteries, showed a uniform diameter of 200 nm and an optimal specific surface area (670 m<sup>2</sup>/g), following



498 excellent performance and cycling stability (sustained specific capacity of 942 mA-h/g  
499 for 600 cycles at a 1 A/g).

## 500 *2.6 Catalytic superiority of materials synthesized via Joule heating synthesis*

501 As one kind of high-temperature shock synthesis strategy, Joule heating can avoid  
502 phase separation of materials with complex components, and the macrostructure of the  
503 materials can be maintained. Meanwhile, the particles engaged in the reaction process  
504 tend to be generated in nanometre scale, thus enabling micro-regulation and  
505 improvement of the electronic structure of the material. In terms of catalytic reaction,  
506 the Joule heating offers a superior approach to improve the catalytic activity and  
507 structural stability of the material. In detail, during the catalytic reaction, Joule heating  
508 can improve the electronic structure of the adsorption sites, by inducing and  
509 maintaining defects, which leads to the effective combination of intermediates and  
510 adsorption sites, thus enhancing the catalytic activity of the material<sup>19</sup>. And the Joule  
511 heating enables the formation of single-phase alloys from immiscible elements, thereby  
512 offering a novel strategy for the synthesis of multicomponent catalysts with elemental  
513 synergy effect. Besides, during the reaction process, the high temperature generated  
514 transiently induces a considerable number of heterogeneous interfaces, which  
515 significantly increases the active sites on the surface of catalyst<sup>82</sup>. Furthermore, the  
516 chemical bond between the catalyst and the carrier is also strengthened during the ultra-  
517 fast Joule heating for self-supporting material (such as Ni foam, carbon paper), thus  
518 enhancing the mechanical stability of the catalyst on matrix<sup>43</sup>. It should also be noted

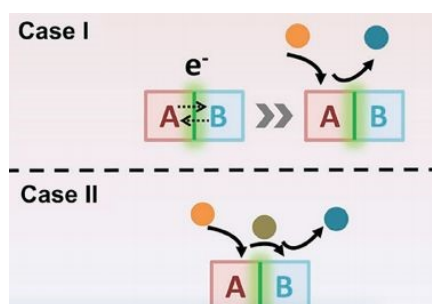
that the rapid heating and cooling process can result in the tendency which transform the catalyst from a stable phase to metastable state, leading to a more enhanced catalytic performance. Therefore, the unique physico-chemical properties endowed by Joule heating highlight the significant potential in synthesizing high active materials, which will be discussed as below.

### 3. Applications of Joule heating in synthesis of highly active catalysts

#### 3.1 Application of Joule heating in interface engineering

In general, an ideal catalyst should be characterized with large specific surface area, electronic conductivity, long-term stability<sup>83</sup>, which contribute to the efficient conversion of energy. Fortunately, the interfacial engineering can optimize the electron transfer process among heterostructures materials and regulate the interface electronic structure via synergistic effect<sup>84-85</sup>. Meanwhile, the interfacial engineering can be applied to improve the stability and long-term performance of catalytic interfaces by designing stable interfacial structures, introducing protective layers or interfacial modifiers<sup>86</sup>. Typically, two mechanisms have been reported, which could effectively facilitate the catalytic activity via interfacial engineering<sup>87</sup>. In case 1, the interface between component A and component B of the catalyst establishes a transport channel for electron transfer, as shown in Fig. 6, wherein the reaction is mainly triggered on component A, thus the catalytic rate can be governed by the binding energy between component A and reactant. It is worth noting that the adsorption and desorption strengths between the catalyst and the reactants can be effectively optimized by inducing

electron modulation through interfacial engineering, which in turn improves the catalytic activity. In contrast to case 1, the component A and B in case 2 is responsible for the adsorption process and the desorption process, respectively. The presence of interface plays an important role in transferring intermediates from A to B.



544

545 *Figure 6 Mechanisms of interfacial engineering effects on catalytic activity. Reproduced with*  
546 *permission.<sup>88</sup> Copyright 2019, Wiley-VCH.*

The conventional methods of materials synthesis are characterized with protracted reaction times and slow heating rate, and the equilibrium thermodynamics among the process render it challenging to generate a number of lattice friction as active interface in catalytic reaction<sup>76, 88</sup>. Fortunately, the rapid heating and quenching rates of Joule heating synthesis can be utilized to generated enormous temperature gradient, wherein the subsequently generated thermal stress can drive the formation of multiple dislocations as high active interface<sup>89-90</sup>. For example, Lai *et al.* successfully prepared Ir-based nanoparticles with abundant Frank partial dislocation (FPDs) as shown in Fig. 7a, wherein the 4% compression was generated compared with standard Ir PDF<sup>89</sup>. In contract, less strain and dislocation could be detected in the Ir particles (Fig. 7b), which was prepared via milder high-temperature calcination method. Meanwhile, the Ir-based

nanoparticles with FPDs synthesized by Joule heating exhibited excellent HER performance (12 mV@10 mA cm<sup>-2</sup> in acid solution) and 2.7 times lower than that synthesized via conventional method. Meanwhile, the rapid Joule heating could avoid the accumulation of active sites, which provides feasible pathway to regulate heterostructure, thus providing abundant catalytic sites in designed catalysts. For example, Zhang *et al.* provided a feasible Joule heating treatment strategy to modulate interfacial structures and properties for rational design of advanced electrocatalysts<sup>91</sup>. In detail, the Joule heating treatment method was applied to modulate the interfacial oxygen species of graded indium oxide nanosheets (Fig. 7c), which was combined with the subsequent in-situ electrochemical reduction process to prepare metal/metal oxide heterostructures (In/In<sub>2</sub>O<sub>3</sub>-1600). And the interfacial structural oxygen species was rationally regulated. Besides, Sun *et al.* designed a well-lattice-matched Co<sub>2</sub>Mo<sub>3</sub>O<sub>8</sub>/MoO<sub>2</sub> heterointerfaces on Ni foam (Co<sub>2</sub>Mo<sub>3</sub>O<sub>8</sub>/MoO<sub>2</sub>/NF) through a rapid Joule heating method<sup>15</sup>. During the Joule heating process, Co<sub>2</sub>Mo<sub>3</sub>O<sub>8</sub>/MoO<sub>2</sub>/NF exposed abundant Co<sub>2</sub>Mo<sub>3</sub>O<sub>8</sub> and MoO<sub>2</sub> compatible interfaces and lattice dislocations (Fig. 7d-f), which can result in electronic rearrangement on the heterogeneous interface, optimizing the activity of active sites. It should be noted that the sample prepared by conventional CVD heating process showed less interfaces due to the prolong heating treatment. Besides, abundant uncoordinated Mo<sup>4+</sup> species could be obtained by the rapid Joule heating process, which was of vital importance to optimize the adsorption behaviour of H<sub>2</sub>O. As a result, Co<sub>2</sub>Mo<sub>3</sub>O<sub>8</sub>/MoO<sub>2</sub>/NF showed excellent HER activity

(23 mV at 10 mA cm<sup>-2</sup>) and stability (100 mA cm<sup>-2</sup> @ 200 h) in seawater splitting wherein the activity of Co<sub>2</sub>Mo<sub>3</sub>O<sub>8</sub>/MoO<sub>2</sub>/NF was much lower than that synthesized by CVD process (56 mV at 10 mA cm<sup>-2</sup>).

The formation of strong interactions between heterogeneous structures represents a crucial factor in significantly enhancing both catalytic activity and stability. Recently, Hu *et al.* designed Ag/Co/C hybrid electrocatalyst with quenched immiscible structure, wherein the formed large immiscibility gap among Ag-Co system, synthesized by ultra-fast heating and cooling, facilitated the strong electronic interaction<sup>92</sup>. Thus, as-prepared Ag/Co/C catalyst exhibited the mass activity of 1.55 A mgAg<sup>-1</sup> at 0.80 V in alkaline solution. Meanwhile, the interfacial engineering also plays an important role in remaining the mechanical stability when working in harsh operation. It is effective to enhance chemical stability through the strategies of tuning electronic structure via rapid Joule heating. For instance, Liu *et al.* utilized instantaneously formed Mo-C bonds between active MoxC and CNT through Joule heating to greatly hinder dissolution and exfoliation of Mo species<sup>82</sup>. The significantly improved charges transfer and binding energy between active MoxC and CNT provided strong coupling. Similarly, to realize the intimate physical contact and low impedance for ion transfer between oxide-based solid electrolytes (SEs) and electrodes, Tour *et al.* applied rapid sintering process based on Joule heating to fabricate ion-conductive SE-cathode interphase within 10 s<sup>93</sup>. Compared with the conventional physical contact of SE-cathode interphase, the rapid sintering reaction could obtain the SE-cathode interphase with well-combination,

600 wherein the  $\text{LiCoO}_2$  and  $\text{Li}_{1.3}\text{Al}_{0.3}\text{Ti}_{1.7}(\text{PO}_4)_3$  merged into monolith as shown in Fig. 7g,  
601 Meanwhile, the grain boundary growth between  $\text{Li}_{1.3}\text{Al}_{0.3}\text{Ti}_{1.7}(\text{PO}_4)_3$  and electrode was  
602 facilitated. Sun *et al.* synthesized a series of  $\text{Li}_{1.3}\text{Al}_{0.3}\text{Ti}_{1.7}(\text{PO}_4)_3$  (LATP)-based solid-  
603 state batteries via thermal pulse sintering (TPS) and conventional furnace sintering (FS)  
604 to investigated important role in high-energy-density solid-state batteries (SSBs)<sup>94</sup>. As  
605 shown in Fig. 7h and i, the TPS technique based on the Joule heating not only improved  
606 the ionic conductivity of LATP ( $8.20 \times 10^{-4} \text{ S cm}^{-1}$ ), but also endowed LATP with  
607 enhanced density to facilitate interfacial contact. Meanwhile, the LATP could realize  
608 the structural evolution under the TPS methods, thus synthesizing extra  $\text{Li}^+$  conduction  
609 pathways as shown in Fig. 7j, wherein the universality of TPS was also verified Fig. 7k  
610 and l.

611 In conclusion, rational design of interfacial engineering via Joule heating provides a  
612 new strategy to effectively optimize the electronic structure as well as heterointerfaces  
613 among catalysts.

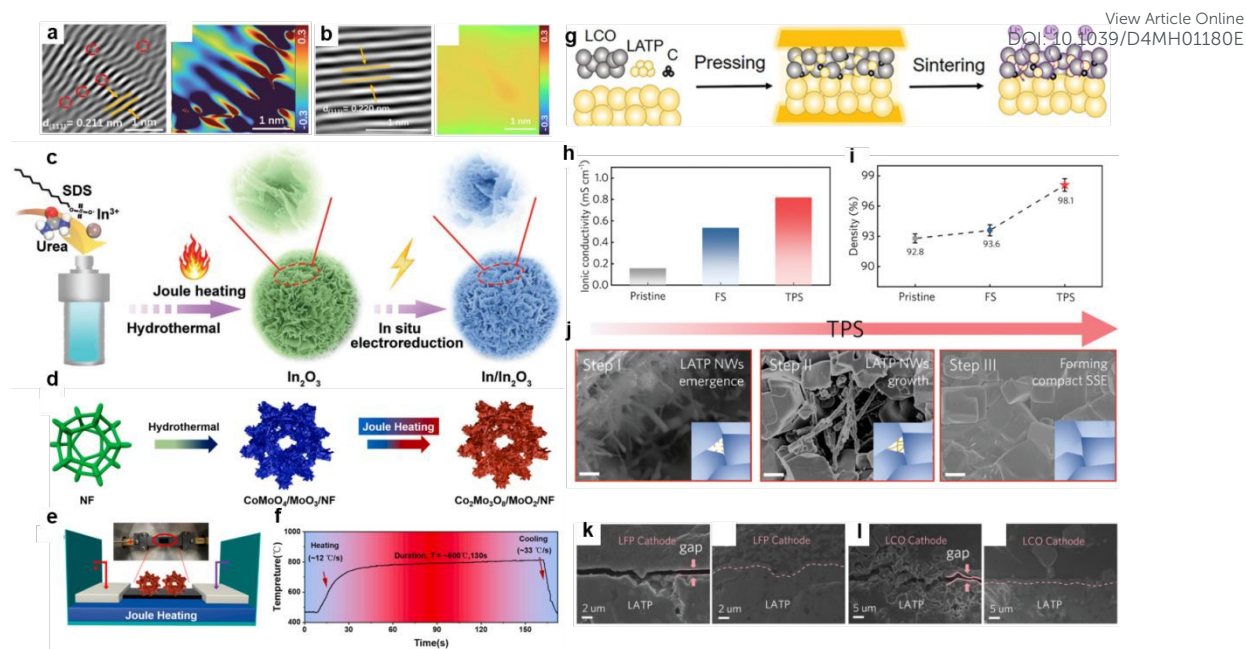


Figure 7 The IFFT patterns and strain distributions of Ir-based sample synthesized via (a) Joule heating and (b) conventional high temperature calcination. Reproduced with permission.<sup>89</sup> Copyright 2023, Wiley-VCH. (c) The schematic synthesis of In/In<sub>2</sub>O<sub>3</sub> via Joule heating method. Reproduced with permission.<sup>91</sup> Copyright 2022, Wiley-VCH. (d) The schematic synthesis of Co-O-Mo heterostructure via Joule heating method. (e) Schematic diagram of Joule heating setup. (f) The heating curves of Joule heating. Reproduced with permission.<sup>15</sup> Copyright 2023, Elsevier. (g) The schematic synthesis of electrode based on the Joule heating. Reproduced with permission.<sup>93</sup> Copyright 2024, Wiley-VCH. The measured ionic conductivity (h) and densities (i) for the LATP inorganic solid electrolyte based on different synthesis methods. (j) The SEM images of LATP treated via thermal pulse sintering. (k) The SEM images of LiFePO<sub>4</sub> and LiCoO<sub>2</sub> cathode/SSE interface with/without thermal pulse sintering. Reproduced with permission.<sup>94</sup> Copyright 2024, Wiley-VCH.

### 3.2 Application of Joule heating in synthesis of nanoparticles

Nanoparticles are specialized materials with sizes typically in the nanoscale, which exhibit unique properties due to the size-dependence and have attracted much attention in the field of catalysis<sup>49</sup>. The precise control of the size and composition of the metal

631 nanoparticles on the support can be achieved by finely tuning the synthesis parameters  
632 to ensure the suitability and controllability of the nucleation process. However,  
633 conventional synthesis methods, such as long-term pyrolysis, hydrothermal method,  
634 electrodeposition are characterized with prolonged treatment and slow heating rate,  
635 which may lead to the inevitable aggregation of active sites and weak electronic  
636 interaction among particles and substrate, thus causing the deteriorated catalytic  
637 activity. Fortunately, the use of Joule heating method enables the rapid synthesis of  
638 uniformly sized nanoparticles and the regulation of nanoparticle size by adjusting the  
639 temperature and duration of the Joule thermal action (10 ms to 10 s)<sup>95</sup>.

640 The rational design of nanoparticles-based materials, via rapid Joule heating method,  
641 has been widely reported as the following guidelines: Firstly, the design of ultra-small  
642 size of nanoparticles can reduce unnecessary bulk atoms in the catalytic reaction  
643 comparing to conventional nanoparticle catalysts, which also exhibits high intrinsic  
644 activity. Yao *et al.* realized the uniformly dispersed metallic ultra-small nanoclusters  
645 (< 2 nm) on defective substrates via rapid Joule heating<sup>96</sup>. In detail, the particle  
646 synthesis duration of rapid Joule heating could be well adjusted in the millisecond scale,  
647 thus avoiding the particle coarsening. Similarly, Hu *et al.* showed that high entropy  
648 alloy (HEA) catalysts with a homogeneous mixture of multiple elements were  
649 successfully prepared by rapid heating and cooling of the metal precursor on the carbon  
650 carrier (Fig. 8a), which exhibited well-dispersibility. The method utilized rapid thermal  
651 shock (~2000 K, duration: 55 ms, ramp rate: ~10<sup>5</sup> K/s) to effectively alloy eight



incompatible elements in nanoparticle (Fig. 8b), breaking through the limitations of conventional synthesis techniques<sup>14</sup>. For comparison, the samples have been treated by the conventional reduction procedures, which tended to exhibited phase-separated heterostructures. And based on the generous adjustable parameters and duration of heating for Joule heating, the concentration of surface-bound residual oxygen on the surface of CNF has been proved to affect the particle fission and corresponding dispersity. This synthesis method has shown great utility in the preparation of multi-membered HEA-nanoparticle catalysts for ammonia oxidation reactions, achieving nearly 100% conversion and more than 99% NO<sub>x</sub> selectivity.

In addition, ultra-small based nanoparticles catalysts not only provide a large number of active sites for activation of various intermediates, but also maintain an efficient utilization rate, making all highly dispersed nanoparticles available for adsorption and conversion of reactants. *Zhao et al.* utilized rapid Joule heating to decompose the Ni-O-Mo precursor (Fig. 8c) to dense MoNi<sub>4</sub> nano-particles on MoO<sub>2</sub> nanorods (MoNi<sub>4</sub>/MoO<sub>x</sub>) (Fig. 8d)<sup>17</sup>. The rapid heating/cooling rates endowed catalysts with larger specific surface area, smaller nano-particles and larger electrochemical area comparing with the catalysts synthesized by traditional calcination (MoNi<sub>4</sub>/MoO<sub>x</sub>-T) (Fig. 4e). Meanwhile, the increased Mo<sup>4+</sup> species in the MoNi<sub>4</sub>/MoO<sub>x</sub> with rapid Joule heating has been proved, which was characterized with low empty d-orbital density and rendered optimized adsorption between \*H and Mo species. As a result, the MoNi<sub>4</sub>/MoO<sub>x</sub> exhibited ultralow potential for the hydrogen evolution reaction in

seawater ( $15\text{ mV @ }10\text{ mA cm}^{-2}$ ), which was much superior than that of  $\text{MoNi}_4/\text{MoOx}$ -  
T. Meanwhile, it should be noted that the rapid Joule heating method saved  $\sim 99\%$   
energy among the synthesis process compared with the traditional calcination,  
indicating the potential in the aspect of low-cost. Besides, Zhao *et al.* alloyed Mo with  
suitable Ru species via Joule heating to generate RuMo nanoparticle ( $\sim 3\text{ nm}$ ) on  $\text{MoOx}$ ,  
which not only elevated Mo-O\* antibonding level by the rational introduction of  $\text{Ru}^{43}$ ,  
thus inhibiting oxidative release of Mo among large current density ( $2000\text{ h @ }1000$   
 $\text{mA cm}^{-2}$ ), but also was beneficial to water splitting through the synergistic effect.  
Meanwhile, it should be noted that the Joule heating synthesis played an important role  
in rational control of morphology and active sites, wherein the effective protons transfer  
kinetics has also been improved in term of hydrogen spillover.

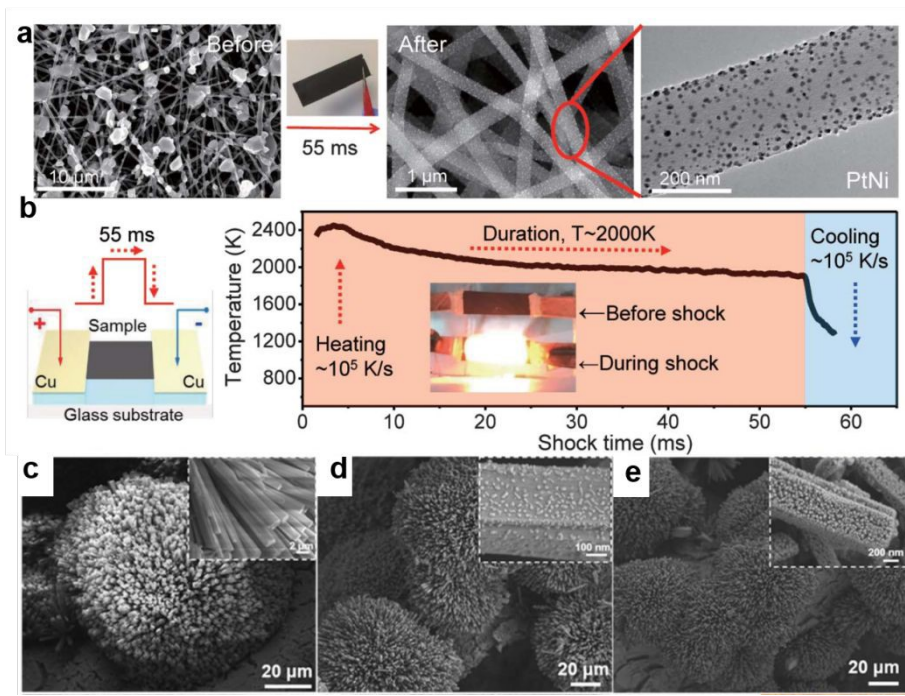


Figure 8 (a) The image precursor salt on the support (before) and the well-dispersed nanoparticles on the support (after) synthesized by Joule heating method. (b) The schematic

synthesis of catalyst via Joule heating method. Reproduced with permission.<sup>14</sup> Copyright

2018, American Association for the Advancement of Science. The scanning electron

microscope image of (c) Ni-O-Mo precursor, (d) MoNi<sub>4</sub>/MoO<sub>x</sub> synthesized by Joule heating

and (e) MoNi<sub>4</sub>/MoO<sub>x</sub>-T synthesized by traditional heating. Reproduced with permission.<sup>17</sup>

Copyright 2023, The Royal Society of Chemistry.

### 3.3 Application of Joule heating in synthesis of single atoms based-catalysts

The concept of single-atom catalysts (SACs) originated in 2011, when Zhang *et al.* successfully prepared iron oxide (FeO<sub>x</sub>)-loaded single-atom platinum (Pt) catalysts (Pt<sub>1</sub>/FeO<sub>x</sub>) and demonstrated that single Pt atoms coupled with FeO<sub>x</sub> carriers had excellent catalytic activity for carbon monoxide (CO) oxidation<sup>97</sup>. Since then, SACs have become a research hotspot in the field of heterogeneous catalysis and have received extensive attention in the past decades<sup>98</sup>. Generally, the SACs consisting of isolated individual metal atoms that are uniformly dispersed on the surface of solid carrier without direct interaction with each other<sup>99</sup>. SACs can be categorized into various types, including metal single atoms anchored to metal oxide surfaces, metals, carbon-based materials, metal-organic frameworks (MOFs), covalent organic frameworks (COFs), and composites<sup>100</sup>. Typically, SACs have been considered as one of the hottest catalytic materials due to the maximum atom utilization efficiency, low coordination metal centers and strong metal-carrier interactions<sup>101</sup>. Unlike conventional nanoparticle-based catalysts, the metal atoms of SACs are highly dispersed on the carrier, which can form bonds with only a few atoms or groups on the carrier, thus leading to the lower coordination number of atoms than bulk phase, wherein the low-

coordination environment in the catalytic center is more conducive to the interaction of active sites with reactant molecules<sup>100</sup>. In addition, the coordinating atoms can effectively optimize the electronic structure of the active center atoms and improve the selectivity of the reaction with the 100% atom utilization (Fig. 9)<sup>102</sup>.

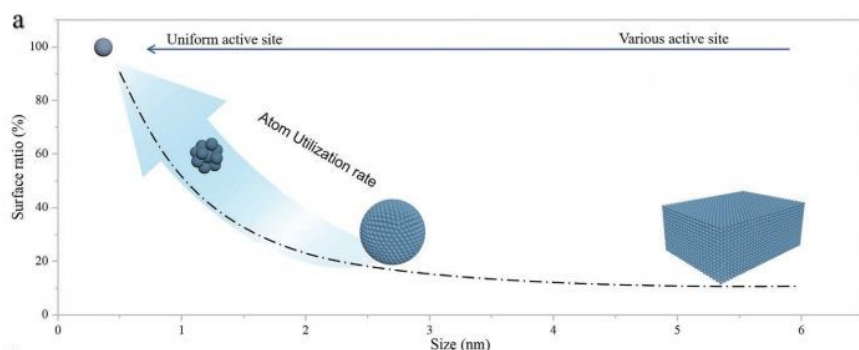


Figure 9 Schematic illustration of surface ratio of atoms at different particle sizes.

Reproduced with permission.<sup>102</sup> Copyright 2024, Wiley-VCH.

However, the SACs also suffer from the shortcoming that the dramatically increased specific surface area in single-atom level leads to a sharp increase of free energy of the metal surface. The subsequent tendency to agglomerate during synthesis and catalytic processes seriously affects the practical application of SACs. The high temperature pyrolysis (HT) has been demonstrated to facilitate the bond formation between metal atoms and substrates with single-atom stabilization and dispersion<sup>103</sup>. However, the prolong HT can induce the particle migration and coalescence (PMC) and Ostwald ripening mechanisms (OR), which are driven by the Brownian motion and the difference of free energy on the surface, respectively<sup>104</sup>. Thus, the conventional HT methods with prolong treatment and slow heating rate, such as chemical vapor deposition, suffer from the undesired phase segregation and the atomic agglomeration,

727 which limits the synthesis and application of SACs. Fortunately, the Joule heat can  
728 realize a rapid temperature increase up to 3000 °C in a short period of time (0-1 s) to  
729 achieve an ultrafast thermal shock effect<sup>38</sup>, which enhances the stability of single-atom  
730 catalysts. Specifically, the rapid ignition with ultra-short heating treatment can  
731 effectively prevent atomic diffusion and agglomeration, which also avoids the  
732 destruction of substrates such as Ni foam and carbon cloth. Recently, *Yao et al.* reported  
733 that single atoms can be effectively synthesized and stabilized at high temperatures  
734 (1500-2000 K) via a Joule heat-controllable high-temperature shockwave methods (Fig.  
735 10a), which was achieved by a programmable periodic on-off heating mode with a short  
736 treatment (e.g.,  $\sim 1,500\text{ K} \leq 55\text{ ms}$ ). The thermodynamically stable metal defect bonds  
737 could be formed. Typically, the rapid heating provided activation energy for  
738 monoatomic dispersion, and the off-state critically ensured overall stability, especially  
739 for the substrate. It should be noted that the reported shockwave approach is  
740 characterized with simplification, ultrafast rates, and versatility (e.g., Pt, Ru, and Co  
741 elements, as well as carbon, C<sub>3</sub>N<sub>4</sub>, and TiO<sub>2</sub> substrates), which provides a platform for  
742 the SACs fabrication<sup>105</sup>.

743 The catalytic activity of SACs is related with the unique local coordination environment  
744 between the isolated atom and carrier<sup>106</sup>. And recent researches have proved the role of  
745 Joule heating in regulating the coordination and electronic states of SACs, which is  
746 superior to conventional methods. For example, *Jiang et al.* reported a thermal shock  
747 (TS) methods to tune the local environment of isolated Pt<sup>2+</sup> for yielding highly active

748 and thermally stable  $\text{Pt}_1/\text{CeO}_2$  catalysts<sup>106</sup>. Typically, an ultrafast shock wave (>  
749 1200 °C) induced the surface remodeling of  $\text{CeO}_2$  to generate Pt single atoms with  
750 asymmetric  $\text{Pt}_1\text{O}_4$  structure in the inert atmosphere. Due to this unique coordination,  
751  $\text{Pt}_1^{\text{d}+}$  is in a partially reduced state during CO oxidation, resulting in excellent low-  
752 temperature performance. Compared with the Atom trapping method (AT), the Joule  
753 heating, with ultrafast shockwave, exhibited potential in modulating the electronic  
754 structure of the adsorption sites, wherein the near-perfect square-planar  $\text{Pt}_1\text{O}_4$   
755 coordination synthesized with AT limited the potential of Pt active sites as shown in  
756 Fig. 10b. Similarly, *Zhang et al.* constructed Pt SAs immobilized on monolayer  
757  $\text{Ti}_3\text{C}_2\text{Tx}$  sheets  $\text{O}_\text{V}$  by rapid thermal shock technique. During the heating treatment, the  
758 Pt species was reduced to metallic state and coordinated with the positively charged  
759 local environment driven by the rapid thermal shock technique. And the resulting  
760  $\text{Ti}_3\text{C}_2\text{Tx-Pt}$  SA catalysts exhibited excellent hydrogen evolution reaction (HER)  
761 performance compared to 20 wt% Pt/C catalysts with good stability (1000 cycles or 89  
762 h)<sup>107</sup>. The above researches indicate that the rapid Joule heating not only avoid  
763 undesired phase segregation and the atomic agglomeration during the synthesis process,  
764 but also effectively modulate the local coordination environment of SACs, which  
765 exhibits potential in terms of regulation of SACs compared with conventional methods.



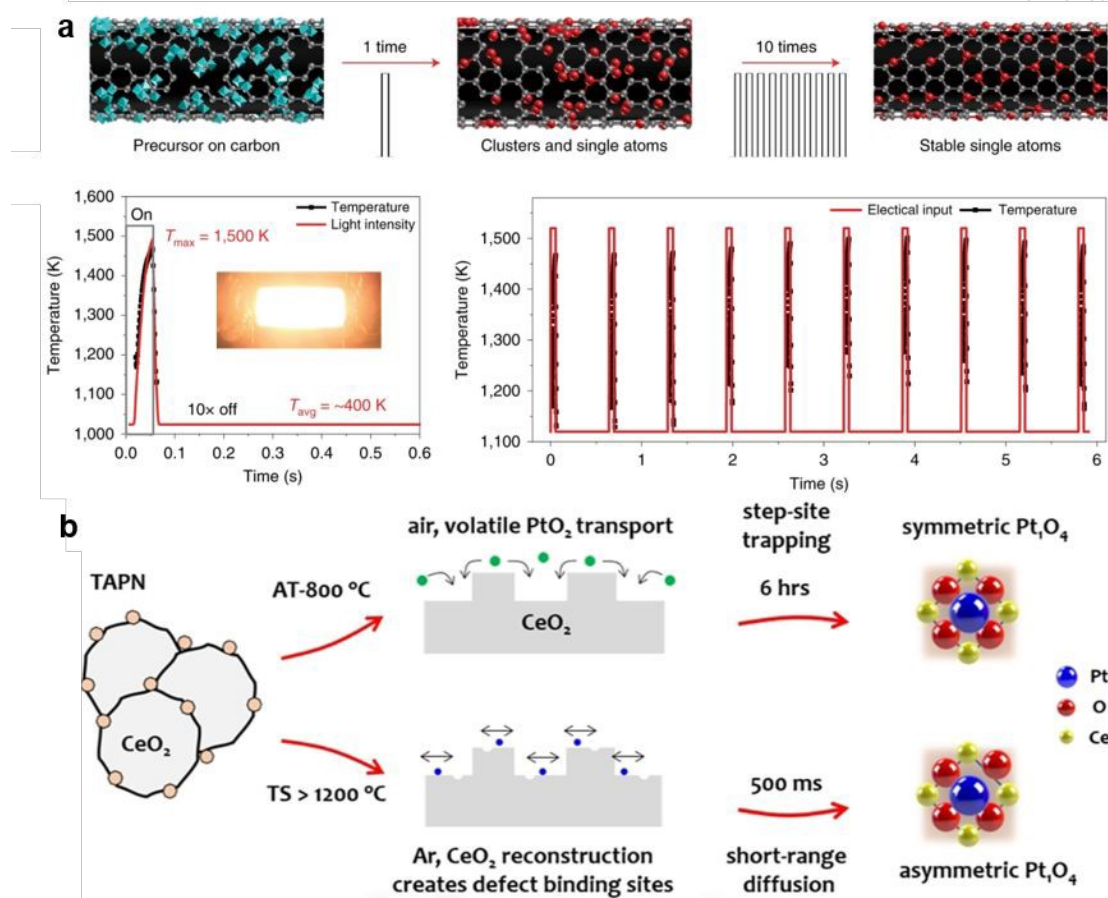


Figure 10 (a) Schematic illustration of the synthesis of catalyst via Joule heating method with the heating/cooling curves. Reproduced with permission.<sup>106</sup> Copyright 2019, Nature. (b) Schematic illustration of the rapid Joule heating process and AT method applied on treatment of precursor. Reproduced with permission.<sup>107</sup> Copyright 2021, Wiley-VCH.

### 3.4 Application of Joule heating in synthesis of high entropy compound

High-entropy materials (HEMs) are single-phase novel electrocatalysts consisting of five or more uniformly distributed metal elements, which provide an ideal platform for tuning the electronic structure and geometrical configuration of metal centres<sup>108</sup>. Typically, the multiple atomic species are uniformly distributed in the same lattice, wherein the catalytic sites can be effectively expanded. In addition, due to the diverse microenvironments and tunable electronic structures, various HEMs such as high

778 entropy alloys (HEAs), high entropy oxides (HEOs) are designed and fabricated for  
 779 improving the catalytic activity<sup>109</sup>, which are characterized with better selectivity,  
 780 stability, and catalytic activity than conventional materials and show good potential for  
 781 development in the field of functional materials<sup>110</sup>. Based on the thermodynamic theory,  
 782 the relation between enthalpy and entropy serves to determine whether HEMs is  
 783 capable of being formed as shown in Eq. 7. And the HEMs is characterized with  $\Delta S_M$   
 784  $\geq 1.5R$ .

$$785 \quad \Delta G = \Delta H - T\Delta S_M \quad (7)$$

786 The  $\Delta S_M$  denotes mixing entropy,  $T$  denotes temperature,  $\Delta H$  denotes enthalpy and  
 787  $\Delta G$  denotes Gibbs free energy, wherein the  $\Delta S_M$  can be calculated as Eq. 8.

$$788 \quad \Delta S_M = \Delta S_M^C + \Delta S_M^V + \Delta S_M^M + \Delta S_M^E \quad (8)$$

789 The  $\Delta S_M$  denotes mixing entropy,  $\Delta S_M^C$  denotes configurational entropy,  $\Delta S_M^V$   
 790 denotes vibrational entropy,  $\Delta S_M^M$  denotes magnetic dipole entropy and  $\Delta S_M^E$  denotes  
 791 electronic randomness entropy. Meanwhile, the configurational entropy can be  
 792 calculated as Eq. 9 and is the dominant component in mixing entropy.

$$793 \quad \Delta S_M^C = k \ln W = R \left( \frac{1}{N} \ln N + \dots + \frac{1}{N} \ln N + \frac{1}{N} \ln N \right) = R \ln N \quad (9)$$

794 The  $W$  represents the confusion degree,  $k$  denotes the Boltzmann constant.  $N$  and  $R$   
 795 are the number of near-equi-molar ratio elements and molar constant, respectively.

796 According to the Eq. 6, the enthalpy plays an important role in the formation of HEMs,  
 797 and the enthalpy of element interaction is subjected to the nature of contained elements,



798 which determines the formed phase under near-equilibrium condition as shown in Fig.  
799 11a. Therefore, the near-zero value of  $\Delta H$  can facilitate the formation of HEMs with  
800 the domination of entropy, wherein the elements can co-exist without attraction and  
801 repelling<sup>111</sup>. However, previously reported synthesis methods are mainly based on  
802 thermal treatment via tube furnaces, which requires long heating, holding and cooling  
803 processes. Thus, it is challenging to overcome the large physicochemical differences of  
804 different elements, leading to the high enthalpy and formation of phase-segregated  
805 structures. Meanwhile, the prolonged pyrolysis at high temperatures tends to lead to  
806 agglomeration and sintering of the particles. And the relatively complex synthesis  
807 conditions can cause low nanoparticle loading. In recent years, the preparation of HEMs  
808 by rapid Joule heating has received much attention, which has emerged as a promising  
809 method for the synthesis of a wide range of catalysts due to its ultrafast heating and  
810 cooling rates as shown in Fig. 11b. It should be noted that the cooling rate plays an  
811 important role in the degree of nonequilibrium and structural ordering as shown in Fig.  
812 11c<sup>112</sup>. Meanwhile, the Joule heating also allows for precise heating control in a short  
813 period of time, thus leading to instantaneous formation of nano-sized homogeneous  
814 phases of disordered metal elements. Recently, the HEMs, synthesized by rapid Joule  
815 heating, have been widely investigated in catalytic reaction due to the highly synergistic  
816 effect of high entropy, lattice distortion, slow diffusion, and cocktail effect<sup>113</sup>.

817 Firstly, HEOs are emerging as a class of materials consisting of multiple major metal  
818 elements<sup>114</sup>. Since the unique properties of HEOs endowed by the enhanced entropic

819 contributions, it is necessary to explore new element combinations of HEOs through  
820 rapid high-throughput synthesis techniques<sup>111</sup>. For example, Wang *et al.* synthesised a  
821 carbon substrate by rapid heating using Joule heat for the OER process, which resulted  
822 in a high density and homogeneous dispersion of ultra-small HEOs on the carbon  
823 substrate (Fig. 11d)<sup>115</sup>. The prepared (FeCoNiRuMn)<sub>3</sub>O<sub>4-x</sub> catalysts owned low  
824 overpotentials of only 230 mV and 270 mV to achieve current densities of 10 mA cm<sup>-2</sup>  
825 and 100 mA cm<sup>-2</sup>, which provided a practical and feasible method for the rapid and  
826 efficient preparation of large quantities of homogeneous, high-density, and ultra-small  
827 nanoparticles (Fig. 11e-g).

828 Besides, the HEAs, synthesized via Joule heating, have also attracted increasing  
829 attention from both theoretical and experimental perspectives. For instance, Lin *et al.*  
830 synthesised the multi-electronic metals Cr and Mo by incorporating them into a highly  
831 active NiCoFe framework via a rapid Joule heating method (Fig. 11h)<sup>116</sup>, which is  
832 characterized with uniformly distributed nanoparticles. The catalyst exhibited excellent  
833 OER performance that achieved a current density of 10 mA cm<sup>-2</sup> with only 260 mV  
834 (Fig. 11i and j). In conclusion, the rapid Joule heating method provides a practical and  
835 feasible method for the rapid and efficient preparation of a large number of well-  
836 distributed, high-density HEM.

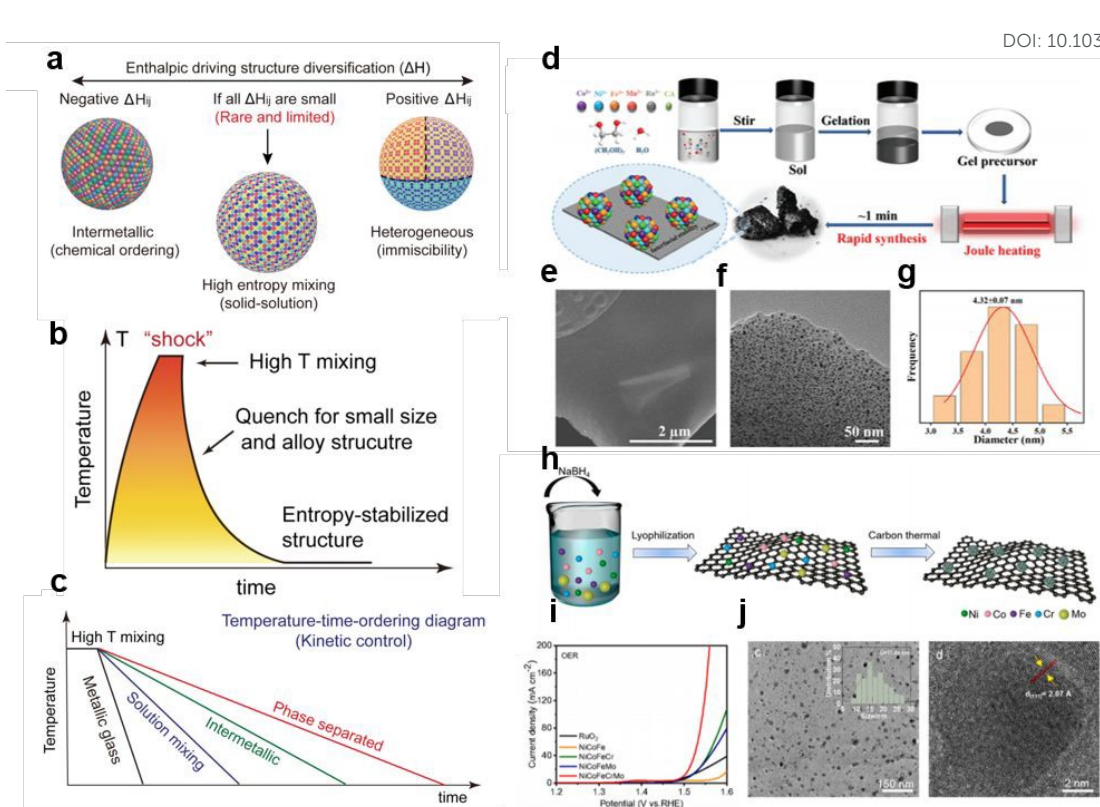


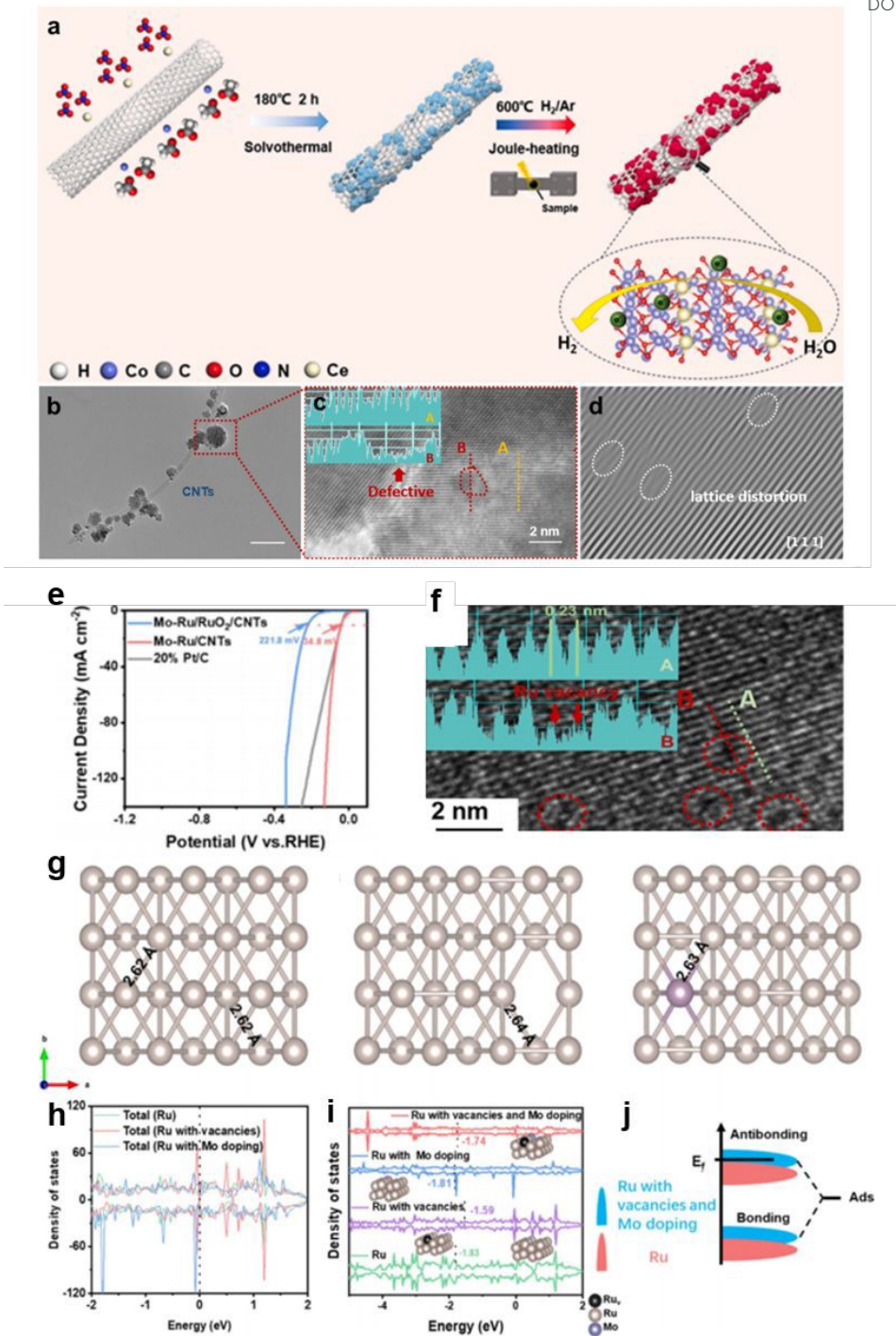
Figure 11 (a) Thermodynamic analysis of HEMs, (b) Schematic illustration of the heating/cooling rate for Joule heating, (c) Temperature-time-transformation diagram. Reproduced with permission.<sup>111</sup> Copyright 2022, AAAS. (d) Schematic illustration of the rapid Joule heating process applied on gel precursor and corresponding HEOs products, (e) SEM image, (f) TEM image, (g) nanoparticle size distribution of the catalyst, Reproduced with permission.<sup>115</sup> Copyright 2024, The Royal Society of Chemistry. (h) Concise illustration of the synthetic route for NiCoFeCrMo HEA nanoparticles, (i) OER polarization curves, (j) TEM images of NiCoFeCrMo HEA nanoparticles. Reproduced with permission.<sup>116</sup> Copyright 2023, Elsevier.

### 3.5 Application of Joule heating in synthesis of defect Engineering

Manufacturing defects is important for improving the electrocatalytic performance of catalysts<sup>117</sup>, especially for carbon-based catalysts<sup>118</sup>. Generally, defects in carbon-based catalysts are generated by doping of heteroatoms or in the conjugated network that lead

851 to anomalous sites (*e.g.* vacancies/holes, edge or topological defects)<sup>119-120</sup>. The  
852 resulting defects cause significant changes in the electron density distribution of  
853 materials, which potentially enhances electron transfer and electron exchange with  
854 exogenous substances, leading to the formation of more active catalytic centres<sup>121-122</sup>.  
855 However, the construction of surface defects tends to lead to the collapse of the material  
856 structure, which is considered as an unfavourable factor in the electrocatalytic  
857 process<sup>123</sup>. The prolonged heating of the traditional heating method tends to cause  
858 surface agglomeration and structural collapse of the catalyst, while the rapid heating  
859 and cooling process of the rapid Joule heating method leads to structural deformation  
860 and lattice strain and the construction of a large number of defects, which provide  
861 abundant active sites with well structural stability<sup>46</sup>. For instance, Li *et al.* succeeded in  
862 the construction of Ce-doped Co/CoO heterojunctions on CNTs by rapid Joule heating  
863 method (Fig. 12a)<sup>47</sup>, and the presence of defects was proved by TEM characterisation  
864 (Fig. 12b-d). The prepared Ce-Co/CoO@CNTs exhibited low overpotentials (47.6 mV  
865 @ 10 mA cm<sup>-2</sup>) in 1 M KOH electrolyte, which was much lower than that of Ce-  
866 Co/CoO@CNTs (T) (362.7 mV) prepared by traditional heating method, indicating the  
867 significant role of Joule heating in engineering defects. As a result, Ce-Co/CoO@CNTs  
868 exhibited a larger electrochemically active surface area and superior intrinsic activity  
869 with a Faraday efficiency close to 100%, demonstrating that the construction of  
870 defective engineering by rapid Joule heating method is of great promise. Besides, Sun  
871 *et al.* prepared superior electrocatalysts (Mo-Ru/CNTs) with cation-rich vacancies Mo-

872 doped Ru nanoparticles on carbon nanotubes by rapid Joule heating<sup>46</sup>, wherein the Mo-  
873 Ru/CNTs exhibited excellent HER activity in alkaline/seawater with only 34.8 mV/44.9  
874 mV at 10 mA cm<sup>-2</sup> (Fig. 12e). Compared with the sample synthesized via CVD methods,  
875 the available vacancy and abundant lattice dislocations in Mo-Ru/CNTs could be  
876 detected as shown in Fig. 12f, while the conventional CVD methods inevitably lead to  
877 the oxidation of Ru species due to the prolong heating. Theoretical analyses indicated  
878 that Ru vacancies and Mo doping on Ru nanoparticles, facilitated by rapid Joule heating,  
879 can modulate the Ru-Ru bond, optimize the d-orbital electronic structure and d-band  
880 centre, thus promoting the adsorption of H\* on the Ru sites (Fig. 12g-j)<sup>124</sup>. Meanwhile,  
881 the TDOS of Ru with vacancies and Mo doping was higher than that of pure Ru,  
882 suggesting that the rapid Joule heating could effectively modulate the electronic  
883 structure and endow materials better conductivity<sup>125-126</sup>.



884

885 Figure 12 (a) Schematic illustration of the synthesis of Ce-Co/CoO@CNTs, (b) TEM image,  
886 (c-d) HRTEM image, Reproduced with permission.<sup>47</sup> Copyright 2024, Elsevier. (e) HER  
887 polarization curves, (f) HRTEM image, (g) Phase models of Ru, Ru with vacancies and Ru  
888 with Mo doping, (h) TDOS, and (i) the d-band center of Ru, (j) Scheme of the electron



configuration of the Ru d-band center. Reproduced with permission.<sup>46</sup> Copyright 2023, The Royal Society of Chemistry.

Besides, offering a flexible electron environment via effective modulation strategy has been widely used to improve the performance of various reaction. Generally, it should be noted that the coordination environment of the active sites can be significantly modulated by the induced defects, which plays an important role in optimizing the electronic structure of targeted active sites and facilitating the activation of adsorbed reactants<sup>127</sup>. Meanwhile, defective substrate surface can effectively form the lattice strain, wherein the bonding between loaded active sites (such as single atom, cluster) and designed support may contribute to the strong electron-metal-support interactions, thus leading to well-dispersion and stabilization of the active sites. For instance, Ren *et al.* deposited active Ru clusters on the BiVO<sub>4</sub> as shown in Fig. 13a, wherein the rapid Joule heating setup has been used to design oxygen vacancies-rich substrate and promoted the formation of Ru clusters<sup>24</sup>. In detail, the rapid heating and quenching processes could effectively maintain the structure of the Ru/BiVO<sub>4</sub>-V<sub>O</sub>, which avoided the aggregation of active metals (about 1.8 nm), thus facilitating the exposed active site. It is vital to note that the induced unsaturated V sites due to the formed oxygen vacancy via Joule heating and modulated Ru clusters played an important role for N<sub>2</sub> adsorption and activation. Moreover, the bonding between Ru and designed BiVO<sub>4</sub> support contributed to the metal-support interactions, thus resulting intense charge redistribution and reducing energy barrier of N<sub>2</sub> fixation reaction. Similarly, Zhao *et al.* innovatively applied specific-size SiO<sub>2</sub> as a hard template to form porous honeycomb

911  $C_3N_4$ , and precisely prepared Ni-doped  $C_3N_4$  via a controllable Joule heating method  
912 as shown in Fig. 13b<sup>19</sup>. Typically, after following Joule heating treatment, the as-  
913 prepared catalysts maintained the 3D structure, which also showed compact structure  
914 characterized with thinner walls (Fig. 13c), indicating the important role of rapid Joule  
915 heating treatment in avoiding the polymerization process. Besides, abundant nitrogen  
916 vacancies were endowed by the rapid heating/cooling rates, wherein the strong  
917 electronic interaction between Ni and nitrogen vacancies was formed. And reducing the  
918 hydrogen adsorption energy of as prepared catalyst was proved by the DFT calculations.  
919 Finally, prepared Ni-doped  $C_3N_4$  exhibited good photocatalytic hydrogen production  
920 performance ( $420.02 \mu\text{mol g}^{-1} \text{h}^{-1} \text{H}_2$  production rate). To improve the synergistic  
921 effect of dual active site with vacancies and active metal sites, Zhao *et al.* also  
922 synthesized Pt metal clusters and N-vacancies co-modified  $C_3N_4$  via Joule heating  
923 method<sup>20</sup>. The Fig. 13d showed a decreased  $N_{2C}$  peak area ratio, indicating that rapid  
924 Joule heating method contributed in constructing nitrogen vacancies, which was  
925 favorable to enhance photocatalytic activity. And the above result was consisted to the  
926 EPR spectra ( $g = 2.0034$ ), wherein the materials treated by fast heating methods tended  
927 to induce more vacancy. Meanwhile, Fig. 13f indicated the Pt species with transferred  
928 to low valent  $\text{Pt}^0$  benefiting from the Joule heating, thus leading to the facilitated  
929 electron transfer between Pt and substrates, which strengthen the performance of  
930 photocatalytic hydrogen production. Finally, The DFT calculations achieved good  
931 agreements with the above conclusion, wherein the hydrogen adsorption energies of



Pt/NV-CN with Pt active sites as well as N vacancy showed low value of 0.41 eV, thus indicated Pt/NV-CN owned excellent proton adsorption and hydrogen adsorption/desorption behavior.

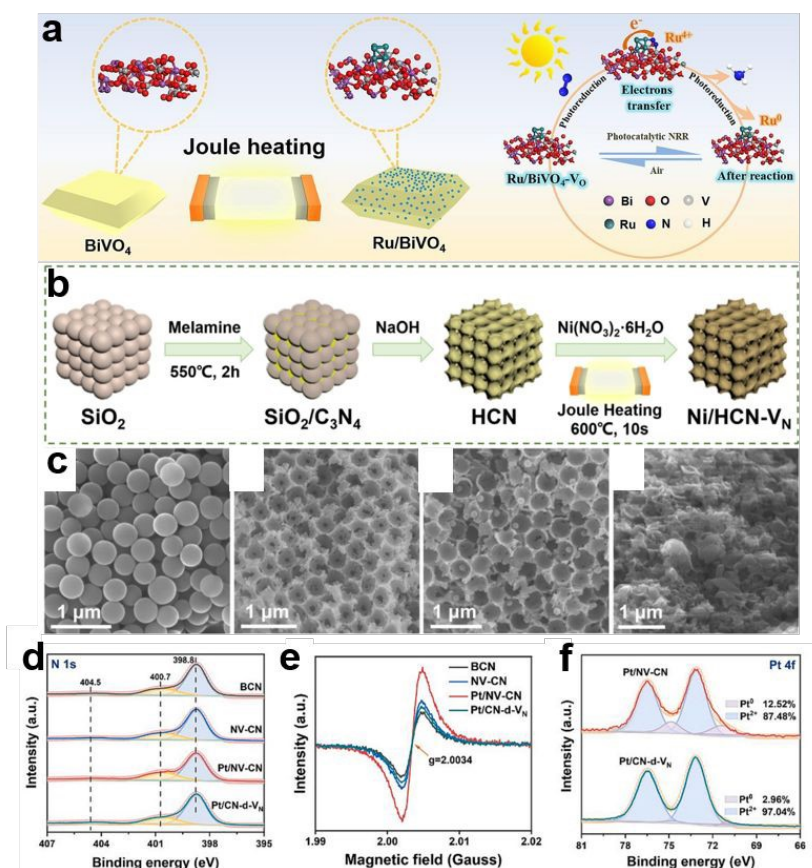


Figure 13 (a) Schematic illustration of the synthesis of Ru/BiVO<sub>4</sub> via Joule heating and the reaction mechanism for photocatalytic N<sub>2</sub> fixation, Reproduced with permission.<sup>24</sup> Copyright 2023, Elsevier. (b) Schematic illustration of the synthesis of Ni/HCN-V<sub>N</sub> via Joule heating, (c) SEM and HRTEM images of SiO<sub>2</sub>, honeycomb C<sub>3</sub>N<sub>4</sub>, Ni-doped porous honeycomb C<sub>3</sub>N<sub>4</sub> with abundant nitrogen vacancies and relevant catalysts prepared in a tube furnace. Reproduced with permission.<sup>19</sup> Copyright 2024, The Royal Society of Chemistry. (d) N 1s XPS spectra, (e) EPR spectra, (f) Pt 4f XPS spectra. Reproduced with permission.<sup>20</sup> Copyright 2023, Elsevier.

## 4. Summary and outlook

In this report, firstly, the equipment setup, basic principles, and advantages of rapid Joule heating on synthesis of effective catalysts are briefly illustrated. Typically, benefiting from the extremely fast heating and quenching rate, the Joule heating method is conducive to prevent active sites from further oxidation and agglomeration in long-term operation, which provides platform for the rational design of high-active catalysts. Consequently, various catalyst-construction strategy (such as heterojunction, well-dispersed nanoparticles, single atom, defect and high entropy alloys) can be effectively realized via Joule heating, and the relevant researches have been reported in this review. Although a number of works based on the rapid Joule heating have been widely reported, there are still several challenges of this method, which should be overcome.

1) Due to the ultrashort processing period of catalysts, it is hard to investigate the forming mechanism of catalysts and the relation between heating parameters and targeted structure, which challenges the in-situ techniques as well as the theoretical computational techniques to understand the catalytic mechanism in depth. Firstly, the critical role of reaction kinetics and mass transport in the Joule heating process remains vague. In detail, the transition of precursor, the removal of noncarbon species and growth rate of target structure should be investigated, wherein the temperature, gas environment, number of pulses and heating time have been proved to affect the materials with different characteristics. For instance, how will the long-range order of multi-element alloys change under different temperature and pulse number? Will the

964 mass transfer on different substrate limit the nucleation of material? Will the heating  
965 rate or gas environment change the coordination environment of SACs? The further  
966 researches based on the rapid Joule heating should focus on the relation between  
967 obtained structure and electronic environment of sample and modulated heating  
968 parameters. Secondly, although it is found that the catalytic properties of samples,  
969 synthesized via rapid Joule heating, is superior to that of conventional pyrolysis  
970 techniques, which was endowed by the extremely fast heating rate (e.g.,  $10^5$  K/s) and  
971 transient cooling. The mechanistic understanding of performance enhancement is  
972 ambiguous. It should be noted that the synthesis parameters need to be set specifically  
973 under the two heating methods, aiming to explore the effect of heating rate as well as  
974 quenching rate by controlling variables. Generally, loading nanoparticles on the carriers  
975 via various methods has been considered as an effective approach to form electronic  
976 metal-support interaction (EMSI)<sup>128</sup>, thus enhancing the interactions between the  
977 carriers and metal atoms, which can modulate the electronic structure and improve the  
978 stability of nanoparticles. Accordingly, selecting suitable precursors and Joule heating  
979 parameters to fabricate functional materials with EMSI will be important research  
980 direction. Finally, the ultra-short treatment and high temperature make the mechanistic  
981 researches based on *in-situ* characterisation technology challenging, wherein the  
982 specific spectrum with ultra-fast response for high temperature resistance coupled with  
983 molecular dynamic simulations close to the real reaction are necessary to understand  
984 the formation mechanism and design advanced functional materials.

985 2) Challenges still exist in precise synthesis of diverse hierarchical and heterostructures.

986 Firstly, the phase transition, size, morphology (hollow, yolk-shell structure etc.) and  
987 loading of active sites of materials should be well-defined by tuning the synthesis  
988 process. In detail, the functional materials synthesized via rapid Joule heating are  
989 universally characterized with nanoparticles, which limit the further application in  
990 various fields. For example, it is difficult to realize the selected crystal planes via the  
991 tuning of heating parameters, which is vital importance for the reduction and oxidation  
992 of reactive intermediates in the photocatalytic reactions. Accordingly, selecting suitable  
993 precursors with template strategy to fabricate materials with various structure and  
994 morphology will be an important research direction for satisfying the needs of different  
995 fields. Besides, the construction of species, during the Joule heating process, for surface  
996 functionalization can be removal from precursors due to the ultra-high temperature,  
997 which further hamper the effective preparation of functional materials. Finally, current  
998 studies based rapid Joule heating methods mainly focus on the high-entropy alloys and  
999 carbon-based compound materials. Therefore, the nanomaterials, such as oxides,  
1000 nitrides, selenides, synthesized via rapid Joule heating with reasonable designing  
1001 heating process should be focused to garnered recognition in the energy storage and  
1002 conversion fields.

1003 3) For the field of rapid synthesis of catalysts, the large-scale preparation via Joule  
1004 heating is still immature, wherein the exposed active sites, catalyst morphology and  
1005 defect concentration may be changed due to the scaling-up effects. And the design of

1006 large-scale reactor as well as operating parameters should be significantly considered.

1007 The rapid Joule heating coupled with roll-to-roll processing technique will be important  
1008 research direction for satisfying large-scale synthesis of functional materials. Besides,  
1009 the homogeneous temperature field should be realized for the large-scale synthesis of  
1010 target sample with specific component and morphology. Therefore, various substrate  
1011 or conductive additives, such as CNT, GO and carbon paper, with unique structure and  
1012 characteristics should be investigated to ensure effective heat conduction and  
1013 dissipation during the rapid heating process. Meanwhile, the reasonable combination of  
1014 precursors and additives or substrates should be studied as an important research  
1015 direction. Generally, the high temperature thermal evaporation of additives or  
1016 substrates at high temperatures inevitably affects the phase composition of the  
1017 synthesised samples, thus hampering the investigation of the mechanism on catalytic  
1018 reaction and synthesis of materials with phase purity. Finally, much larger heating area  
1019 or zone may be required with the increasement of material production via Joule heating,  
1020 which, coupled with high accurate temperature sensor, heating control unit and vacuum  
1021 chamber, causes the high capital costs and operating costs. Thus, the feasibility and  
1022 economic evaluation of large-scale via Joule heating methods are required.

1023 4) Currently, the rapid Joule heating has been applied to facilitate the waste recycling.  
1024 However, there is still a huge challenge to obtain various high-added value materials  
1025 via Joule heating method such as polymers, non-conductive precursors, wherein the  
1026 carbon-based products have been mainly focused. Meanwhile, different kinds of matrix

1027 should be designed according to different precursors and heating parameters. In the  
1028 future, combining the Joule heating methods with treatment of other waste such as  
1029 metallurgical slag and seawater may be the potential research direction.

1030 5) Considering the abundant renewable energy and urgency of carbon neutralization,  
1031 the rapid Joule heating is potential to be extend to the broader thermochemical synthesis,  
1032 wherein the precise control of temperature in millisecond level and ultra-high heating  
1033 rate not only facilitate the effective activation of chemical raw reactants, but also  
1034 modulate the reactive pathways, thus leading to enhanced reactive selectivity. Various  
1035 reactions, such as methane conversion reactions, carbon dioxide conversion and  
1036 ammonia synthesis reaction, can utilize Joule heating to realize the precise energy  
1037 supply, enhance product selectivity and minimise catalyst deactivation. Besides, the  
1038 Joule heating has great potential for precise heat transfer to reaction zone, which is  
1039 beneficial to the effective and highly selective conversion of chemical raw reactants,  
1040 thus exhibiting distinct advantages in thermochemical synthesis.

1041 6) Based on the generous adjustable parameters and duration of heating for Joule  
1042 heating, the machine learning coupled with experiment will be a potential way to  
1043 precisely control the reactive paths and effective synthesis. And such strategy plays an  
1044 important role in avoiding the limitation of regulatory mechanism due to the complexity  
1045 of variables. Systematic investigation of heating parameters, such as temperature, gas  
1046 atmosphere, precursor, substrates and heating/cooling rates, will be needed via machine  
1047 learning to achieve efficient and selective synthesis of desired materials.

1048 In conclusion, the novel Joule heating method presents numerous advantageous  
1049 features and provides a promising pathway to realize an effective catalyst-construction  
1050 strategy, which exhibits tremendous application potentials for effective synthesis and  
1051 design of functional catalysts in different fields.

## 1052 Acknowledgments

1053 This work was financially supported by the Fundamental Research Funds for the  
1054 Central Universities (No: 202441006, 202364004 and 202461025)

## 1055 References

- 1056 1. Jiang, R.; Da, Y.; Han, X.; Chen, Y.; Deng, Y.; Hu, W., Ultrafast Synthesis for  
1057 Functional Nanomaterials. *Cell Reports Physical Science* **2021**, 2 (1).
- 1058 2. Cong, L.; Xie, H.; Li, J. J. A. E. M., Hierarchical structures based on two -  
1059 dimensional nanomaterials for rechargeable lithium batteries. **2017**, 7 (12), 1601906.
- 1060 3. Prieto, G.; Zečević, J.; Friedrich, H.; De Jong, K. P.; De Jongh, P. E. J. N. m.,  
1061 Towards stable catalysts by controlling collective properties of supported metal  
1062 nanoparticles. **2013**, 12 (1), 34-39.
- 1063 4. Huang, W.; Bo, T.; Zuo, S.; Wang, Y.; Chen, J.; Ould-Chikh, S.; Li, Y.; Zhou, W.;  
1064 Zhang, J.; Zhang, H., Surface decorated Ni sites for superior photocatalytic hydrogen  
1065 production. *SusMat* **2022**, 2 (4), 466-475.
- 1066 5. Sun, J.-P.; Zhao, Z.; Li, J.; Li, Z.-Z.; Meng, X.-C., Recent advances in  
1067 electrocatalytic seawater splitting. *Rare Metals* **2022**, 42 (3), 751-768.
- 1068 6. Liu, C.; Chen, Z.; Rao, D.; Zhang, J.; Liu, Y.; Chen, Y.; Deng, Y.; Hu, W. J. S. C.  
1069 M., Behavior of gold-enhanced electrocatalytic performance of NiPtAu hollow  
1070 nanocrystals for alkaline methanol oxidation. **2020**, 64 (3), 611-620.
- 1071 7. Pei, Z.; Zhang, H.; Luan, D.; Lou, X. W., Electrocatalytic acidic oxygen evolution:  
1072 From catalyst design to industrial applications. *Matter* **2023**, 6 (12), 4128-4144.
- 1073 8. Zhao, Z.; Sun, J.; Meng, X., Recent advances in transition metal - based  
1074 electrocatalysts for seawater electrolysis. *International Journal of Energy Research*  
1075 **2022**, 46 (13), 17952-17975.



- 1076 9. Zhao, Z.; Li, Z.; Zhang, Z.; Meng, X., Fe/P dual-doping NiMoO<sub>4</sub> with hollow  
1077 structure for efficient hydrazine oxidation-assisted hydrogen generation in alkaline  
1078 seawater. *Applied Catalysis B: Environment and Energy* **2024**, 347.
- 1079 10. Sun, J.; Ren, G.; Qin, S.; Zhao, Z.; Li, Z.; Zhang, Z.; Li, C.; Meng, X.,  
1080 Reconstruction Co-O-Mo in amorphous-crystalline MoO<sub>x</sub>/Co(OH)<sub>2</sub> interface for  
1081 industry-level active and stable electrocatalytic seawater hydrogen evolution. *Nano*  
1082 *Energy* **2024**, 121.
- 1083 11. Lan, K.; Liu, Y.; Zhang, W.; Liu, Y.; Elzatahry, A.; Wang, R.; Xia, Y.; Al-Dhayan,  
1084 D.; Zheng, N.; Zhao, D. J. J. o. t. A. C. S., Uniform ordered two-dimensional  
1085 mesoporous TiO<sub>2</sub> nanosheets from hydrothermal-induced solvent-confined  
1086 monomicelle assembly. **2018**, 140 (11), 4135-4143.
- 1087 12. Shi, Y.; Huang, W.-M.; Li, J.; Zhou, Y.; Li, Z.-Q.; Yin, Y.-C.; Xia, X.-H. J. N. C.,  
1088 Site-specific electrodeposition enables self-terminating growth of atomically dispersed  
1089 metal catalysts. **2020**, 11 (1), 4558.
- 1090 13. Tang, T.; Jiang, W. J.; Niu, S.; Liu, N.; Luo, H.; Zhang, Q.; Wen, W.; Chen, Y. Y.;  
1091 Huang, L. B.; Gao, F. J. A. F. M., Kinetically controlled coprecipitation for general fast  
1092 synthesis of sandwiched metal hydroxide nanosheets/graphene composites toward  
1093 efficient water splitting. **2018**, 28 (3), 1704594.
- 1094 14. Yao, Y.; Huang, Z.; Xie, P.; Lacey, S. D.; Jacob, R. J.; Xie, H.; Chen, F.; Nie, A.;  
1095 Pu, T.; Rehwoldt, M. J. S., Carbothermal shock synthesis of high-entropy-alloy  
1096 nanoparticles. **2018**, 359 (6383), 1489-1494.
- 1097 15. Sun, J.; Qin, S.; Zhang, Z.; Li, C.; Xu, X.; Li, Z.; Meng, X., Joule heating synthesis  
1098 of well lattice-matched Co<sub>2</sub>Mo<sub>3</sub>O<sub>8</sub>/MoO<sub>2</sub> heterointerfaces with greatly improved  
1099 hydrogen evolution reaction in alkaline seawater electrolysis with 12.4 % STH  
1100 efficiency. *Applied Catalysis B: Environmental* **2023**, 338.
- 1101 16. Zhao, Z.; Sun, J.; Li, X.; Zhang, Z.; Meng, X., Joule heating synthesis of NiFe  
1102 alloy/MoO<sub>2</sub> and in-situ transformed (Ni,Fe)OOH/MoO<sub>2</sub> heterostructure as effective  
1103 complementary electrocatalysts for overall splitting in alkaline seawater. *Applied*  
1104 *Catalysis B: Environment and Energy* **2024**, 340, 123277-123294.
- 1105 17. Zhao, Z.; Sun, J.; Li, Z.; Xu, X.; Zhang, Z.; Li, C.; Wang, L.; Meng, X., Rapid  
1106 synthesis of efficient Mo-based electrocatalyst for the hydrogen evolution reaction in  
1107 alkaline seawater with 11.28% solar-to-hydrogen efficiency. *Journal of Materials*  
1108 *Chemistry A* **2023**, 11 (19), 10346-10359.
- 1109 18. Xiong, G.; Chen, Y.; Zhou, Z.; Liu, F.; Liu, X.; Yang, L.; Liu, Q.; Sang, Y.; Liu,  
1110 H.; Zhang, X.; Jia, J.; Zhou, W., Rapid synthesis of various electrocatalysts on Ni foam  
1111 using a universal and facile induction heating method for efficient water splitting. *Adv.*  
1112 *Funct. Mater.* **2021**, 31 (15), 2009580-2009591.
- 1113 19. Zhao, Z.; Ren, G.; Zhang, Z.; Meng, X.; Li, Z., Rapid Joule heating synthesis of Ni  
1114 doped into porous honeycomb C<sub>3</sub>N<sub>4</sub> with greatly improved photocatalytic H<sub>2</sub>  
1115 production. *Inorganic Chemistry Frontiers* **2024**, 11 (9), 2634-2647.



- 1116 20. Zhao, Z.; Ren, G.; Zhang, Z.; Meng, X.; Li, Z., Rapid Joule heating synthesis of Pt clusters on C<sub>3</sub>N<sub>4</sub> with abundant nitrogen vacancies for highly-efficiently  
1117 photocatalytic H<sub>2</sub> production. *Sep. Purif. Technol.* **2024**, 330. View Article Online  
DOI: 10.1039/D4MH01180E
- 1119 21. Zhao, Z.; Sun, J.; Li, X.; Zhang, Z.; Meng, X., Joule heating synthesis of NiFe  
1120 alloy/MoO<sub>2</sub> and in-situ transformed (Ni, Fe)OOH/MoO<sub>2</sub> heterostructure as effective  
1121 complementary electrocatalysts for overall splitting in alkaline seawater. *Applied  
1122 Catalysis B: Environmental* **2024**, 340, 123277-123294.
- 1123 22. Chen, W.; Li, J. T.; Wang, Z.; Algozeeb, W. A.; Luong, D. X.; Kittrell, C.; McHugh,  
1124 E. A.; Advincula, P. A.; Wyss, K. M.; Beckham, J. L.; Stanford, M. G.; Jiang, B.; Tour,  
1125 J. M., Ultrafast and Controllable Phase Evolution by Flash Joule Heating. *ACS Nano*  
1126 **2021**, 15 (7), 11158-11167.
- 1127 23. Yang, H.; Ren, G.; Li, Z.; Zhang, Z.; Meng, X. J. A. C. B. E.; Energy, Fast Joule  
1128 heating for transformation of Fe-MIL-125 (Ti) to Fe/TiO<sub>2</sub> with enhanced  
1129 photocatalytic activity in N<sub>2</sub> fixation. **2024**, 347, 123795.
- 1130 24. Ren, G.; Zhao, Z.; Li, Z.; Zhang, Z.; Meng, X. J. J. o. C., Rapid Joule-Heating  
1131 fabrication of oxygen vacancies and anchor of Ru clusters onto BiVO<sub>4</sub> for greatly  
1132 enhanced photocatalytic N<sub>2</sub> fixation. **2023**, 428, 115147.
- 1133 25. Dou, S.; Xu, J.; Cui, X.; Liu, W.; Zhang, Z.; Deng, Y.; Hu, W.; Chen, Y., High-  
1134 temperature shock enabled nanomanufacturing for energy-related applications. *Adv.  
1135 Energy Mater* **2020**, 10 (33), 2001331-2001346.
- 1136 26. Liu, Y.; Tian, X.; Han, Y.-C.; Chen, Y.; Hu, W. J. C. J. o. C., High-temperature  
1137 shock synthesis of high-entropy-alloy nanoparticles for catalysis. **2023**, 48, 66-89.
- 1138 27. Jiang, R.; Da, Y.; Zhang, J.; Wu, H.; Fan, B.; Li, J.; Wang, J.; Deng, Y.; Han, X.;  
1139 Hu, W., Non-equilibrium synthesis of stacking faults-abundant Ru nanoparticles  
1140 towards electrocatalytic water splitting. *Applied Catalysis B: Environmental* **2022**, 316.
- 1141 28. Qiu, Y.; Hu, Z.; Li, H.; Ren, Q.; Chen, Y.; Hu, S., Hybrid electrocatalyst Ag/Co/C  
1142 via flash Joule heating for oxygen reduction reaction in alkaline media. *Chemical  
1143 Engineering Journal* **2022**, 430, 132769.
- 1144 29. Xia, D.; Mannering, J.; Huang, P.; Xu, Y.; Li, Q.; Li, H.; Qin, Y.; Kulak, A. N.;  
1145 Menzel, R., Electrothermal Transformations within Graphene-Based Aerogels through  
1146 High-Temperature Flash Joule Heating. *Journal of the American Chemical Society*  
1147 **2024**, 146 (1), 159-169.
- 1148 30. Zhang, H.; Qi, S.; Zhu, K.; Wang, H.; Zhang, G.; Ma, W.; Zong, X. Ultrafast  
1149 Synthesis of Mo<sub>2</sub>C-Based Catalyst by Joule Heating towards Electrocatalytic  
1150 Hydrogen Evolution Reaction *Symmetry* [Online], 2023.
- 1151 31. Shen, P.; Zhao, J.; Gao, Y.; Lin, Y.; Han, Y.; Xu, K., General synthesis of transition  
1152 metal nitride arrays by ultrafast flash joule heating within 500 ms. *Science China  
1153 Chemistry* **2024**, 67 (6), 1976-1982.
- 1154 32. Liao, Y.; Zhu, R.; Zhang, W.; Zhu, H.; Sun, Y.; Chen, J.; Dong, Z.; Lv, R.,  
1155 Transient synthesis of carbon-supported high-entropy alloy sulfide nanoparticles via

- 1156 flash Joule heating for efficient electrocatalytic hydrogen evolution. *Nano Research*  
1157 **2024**, 17 (4), 3379-3389.
- 1158 33. Wang, Y.; Chen, X.; Meng, X.; Li, Z., Joule Heating Synthesis of Cobalt  
1159 Molybdate with Unsaturated Mo<sup>4+</sup> Coordination for Greatly Enhanced Electrocatalytic  
1160 Nitrate Reduction to Ammonia. *ACS Sustainable Chemistry & Engineering* **2024**, 12  
1161 (17), 6762-6773.
- 1162 34. Cui, B.; Zhu, H.; Wang, M.; Zeng, J.; Zhang, J.; Tian, Z.; Jiang, C.; Sun, Z.; Yang,  
1163 H.; Liu, Y.; Ding, J.; Luo, Z.; Chen, Y.; Chen, W.; Hu, W., Intermediate State of Dense  
1164 Ru Assembly Captured by High-Temperature Shock for Durable Ampere-Level  
1165 Hydrogen Production. *ACS Materials Letters* **2024**, 6 (4), 1532-1541.
- 1166 35. Li, J.; Wang, C.; Chen, X.; Zhang, Y.; Zhang, Y.; Fan, K.; Zong, L.; Wang, L.,  
1167 Flash synthesis of ultrafine and active NiRu alloy nanoparticles on N-rich carbon  
1168 nanotubes via joule heating for efficient hydrogen and oxygen evolution reaction.  
1169 *Journal of Alloys and Compounds* **2023**, 959, 170571.
- 1170 36. Yang, H.; Ren, G.; Li, Z.; Zhang, Z.; Meng, X., Fast Joule heating for  
1171 transformation of Fe-MIL-125(Ti) to Fe/TiO<sub>2</sub> with enhanced photocatalytic activity in  
1172 N<sub>2</sub> fixation. *Applied Catalysis B: Environment and Energy* **2024**, 347, 123795.
- 1173 37. Hu, Z.; Huang, L.; Ma, M.; Xu, L.; Liu, H.; Xu, W.; Yang, J., A Quick Joule-  
1174 Heating Coupled with Solid-Phase Synthesis for Carbon-Supported Pd-Se  
1175 Nanoparticles Toward High-Efficiency Electrocatalysis. *Advanced Functional*  
1176 *Materials* **2024**, n/a (n/a), 2405945.
- 1177 38. Luong, D. X.; Bets, K. V.; Algozeeb, W. A.; Stanford, M. G.; Kittrell, C.; Chen,  
1178 W.; Salvatierra, R. V.; Ren, M.; McHugh, E. A.; Advincula, P. A.; Wang, Z.; Bhatt,  
1179 M.; Guo, H.; Mancevski, V.; Shahsavari, R.; Yakobson, B. I.; Tour, J. M., Gram-scale  
1180 bottom-up flash graphene synthesis. *Nature* **2020**, 577 (7792), 647-651.
- 1181 39. Li, Y.; Chen, Y.; Nie, A.; Lu, A.; Jacob, R. J.; Gao, T.; Song, J.; Dai, J.; Wan, J.;  
1182 Pastel, G.; Zachariah, M. R.; Yassar, R. S.; Hu, L., In Situ, Fast, High-Temperature  
1183 Synthesis of Nickel Nanoparticles in Reduced Graphene Oxide Matrix. *Advanced*  
1184 *Energy Materials* **2017**, 7 (11).
- 1185 40. Zhang, L.; Peng, L.; Lu, Y.; Ming, X.; Sun, Y.; Xu, X.; Xia, Y.; Pang, K.; Fang,  
1186 W.; Huang, N.; Xu, Z.; Ying, Y.; Liu, Y.; Fu, Y.; Gao, C., Sub-second ultrafast yet  
1187 programmable wet-chemical synthesis. *Nat. Commun.* **2023**, 14 (1).
- 1188 41. Thanh, N. T. K.; Maclean, N.; Mahiddine, S., Mechanisms of Nucleation and  
1189 Growth of Nanoparticles in Solution. *Chem. Rev.* **2014**, 114 (15), 7610-7630.
- 1190 42. Deng, J.; Li, G.; Yan, D.; Zhang, W.; Feng, K.; Nie, K.; Liu, C.; Lv, X.; Zhong, J.,  
1191 Programmable Wet-Interfacial Joule Heating to Rapidly Synthesize Metastable  
1192 Protohematite Photoanodes: Metal and Lattice Oxygen Dual Sites for Improving Water  
1193 Oxidation. *ACS Catalysis* **2024**, 14 (14), 10635-10647.

- 1194 43. Zhao, Z.; Sun, J.; Li, X.; Qin, S.; Li, C.; Zhang, Z.; Li, Z.; Meng, X., Engineering active and robust alloy-based electrocatalyst by rapid Joule-heating toward amper-  
1195 level hydrogen evolution. *Nat. Commun.* **2024**, *15* (1), 7475-7590. [View Article Online](#)  
1196 DOI: 10.1039/D4MH01180E
- 1197 44. Wyss, K. M.; Li, J. T.; Advincula, P. A.; Bets, K. V.; Chen, W.; Eddy, L.; Silva,  
1198 K. J.; Beckham, J. L.; Chen, J.; Meng, W.; Deng, B.; Nagarajaiah, S.; Yakobson, B. I.;  
1199 Tour, J. M., Upcycling of Waste Plastic into Hybrid Carbon Nanomaterials. *Adv. Mater.*  
1200 **2023**, *35* (16).
- 1201 45. Dong, Y.; Rao, Y.; Liu, H.; Zhang, H.; Hu, R.; Chen, Y.; Yao, Y.; Yang, H., Highly  
1202 efficient chemical production via electrified, transient high-temperature synthesis.  
1203 *eScience* **2024**, *4* (4).
- 1204 46. Sun, J.; Zhao, Z.; Li, Z.; Zhang, Z.; Zhang, R.; Meng, X., Ultrafast carbothermal  
1205 shocking fabrication of cation vacancy-rich Mo doped Ru nanoparticles on carbon  
1206 nanotubes for high-performance water/seawater electrolysis. *Journal of Materials*  
1207 *Chemistry A* **2023**, *11* (41), 22430-22440.
- 1208 47. Li, X.; Zhao, Z.; Meng, X.; Li, Z., Rapid Joule-heating fabrication of Ce-doped  
1209 Co/CoO on carbon nanotubes for efficiently electrocatalytic hydrogen production. *Appl.*  
1210 *Surf. Sci.* **2024**, 669.
- 1211 48. Liu, Y.; Han, Y.; Song, Z.; Song, W.; Miao, Z.; Chen, Y.; Ding, J.; Hu, W.,  
1212 Accelerating the Phase Formation Kinetics of Alluaudite Sodium Iron Sulfate Cathodes  
1213 via Ultrafast Thermal Shock. *ACS Appl. Mater. Interfaces* **2024**, *16* (11), 13828-13838.
- 1214 49. Cui, M.; Yang, C.; Hwang, S.; Li, B.; Dong, Q.; Wu, M.; Xie, H.; Wang, X.; Wang,  
1215 G.; Hu, L., Rapid Atomic Ordering Transformation toward Intermetallic Nanoparticles.  
1216 *Nano Lett.* **2021**, *22* (1), 255-262.
- 1217 50. Ji, Y.; Zhang, H.; Yang, D.; Pan, Y.; Zhu, Z.; Qi, X.; Pi, X.; Du, W.; Cheng, Z.;  
1218 Yao, Y.; Qie, L.; Huang, Y., Regenerated Graphite Electrodes with Reconstructed Solid  
1219 Electrolyte Interface and Enclosed Active Lithium Toward >100% Initial Coulombic  
1220 Efficiency. *Adv. Mater.* **2024**, *36* (19).
- 1221 51. Chen, W.; Salvatierra, R. V.; Li, J. T.; Kittrell, C.; Beckham, J. L.; Wyss, K. M.;  
1222 La, N.; Savas, P. E.; Ge, C.; Advincula, P. A.; Scotland, P.; Eddy, L.; Deng, B.; Yuan,  
1223 Z.; Tour, J. M., Flash Recycling of Graphite Anodes. *Adv. Mater.* **2022**, *35* (8).
- 1224 52. Zhang, X.; Han, G.; Zhu, S., Flash Nitrogen-Doped Carbon Nanotubes for Energy  
1225 Storage and Conversion. *Small* **2023**, *20* (3).
- 1226 53. M.A.S.R. Saadi, P. A. A., Md Shajedul Hoque Thakur, Ali Zein Khater, Shabab  
1227 Saad, Ali Shayesteh Zeraati, Shariful Kibria Nabil, Aasha Zinke, Soumyabrata Roy,  
1228 Minghe Lou, Sravani N. Bheemasetti, Md Abdullah Al Bari, Yiwen Zheng, Jacob L.  
1229 Beckham, Venkataramana Gadhamshetty, Aniruddh Vashisth, Md Golam Kibria,  
1230 James M. Tour, Pulickel M. Ajayan, Muhammad M. Rahman, Sustainable  
1231 valorization of asphaltenes via flash joule heating. *Science Advances* **2022**, *8*, eadd3555.
- 1232 54. Chen, J.; Ma, Y.; Huang, T.; Jiang, T.; Park, S.; Xu, J.; Wang, X.; Peng, Q.; Liu,  
1233 S.; Wang, G.; Chen, W., Ruthenium-Based Binary Alloy with Oxide Nanosheath for

- 1234 Highly Efficient and Stable Oxygen Evolution Reaction in Acidic Media. *Adv. Mater.* **2024**, *36* (26).  
1235
- 1236 55. Yang, W.; Shang, L.; Liu, X.; Zhang, S.; Li, H.; Yan, Z.; Chen, J., Ultrafast  
1237 synthesis of nanocrystalline spinel oxides by Joule-heating method. *Chin. Chem. Lett.*  
1238 **2024**, *35* (11).
- 1239 56. Yang, F.; Deng, P.; He, H.; Hong, R.; Xiang, K.; Cao, Y.; Yu, B.; Xie, Z.; Lu, J.;  
1240 Liu, Z.; Khan, D.; Harbottle, D.; Xu, Z.; Liu, Q.; Tang, Z., Rapid Joule heating-induced  
1241 welding of silicon and graphene for enhanced lithium-ion battery anodes. *Chem. Eng.*  
1242 *J.* **2024**, *494*.
- 1243 57. Ding, X.; He, Z.; Li, J.; Xu, X.; Li, Z., Carbon carrier-based rapid Joule heating  
1244 technology: a review on the preparation and applications of functional nanomaterials.  
1245 *Nanoscale* **2024**, *16* (26), 12309-12328.
- 1246 58. Yan, Q.-L.; Gozin, M.; Zhao, F.-Q.; Cohen, A.; Pang, S.-P., Highly energetic  
1247 compositions based on functionalized carbon nanomaterials. *Nanoscale* **2016**, *8* (9),  
1248 4799-4851.
- 1249 59. Edwards, R. S.; Coleman, K. S., Graphene synthesis: relationship to applications.  
1250 *Nanoscale* **2013**, *5* (1), 38-51.
- 1251 60. Li, T.; Pickel, A. D.; Yao, Y.; Chen, Y.; Zeng, Y.; Lacey, S. D.; Li, Y.; Wang, Y.;  
1252 Dai, J.; Wang, Y.; Yang, B.; Fuhrer, M. S.; Marconnet, A.; Dames, C.; Drew, D. H.;  
1253 Hu, L., Thermoelectric properties and performance of flexible reduced graphene oxide  
1254 films up to 3,000 K. *Nature Energy* **2018**, *3* (2), 148-156.
- 1255 61. Liu, Y.; Li, P.; Wang, F.; Fang, W.; Xu, Z.; Gao, W.; Gao, C., Rapid roll-to-roll  
1256 production of graphene films using intensive Joule heating. *Carbon* **2019**, *155*, 462-468.
- 1257 62. Li, J.; Wang, C.; Chen, X.; Zhang, Y.; Zhang, Y.; Fan, K.; Zong, L.; Wang, L.,  
1258 Flash synthesis of ultrafine and active NiRu alloy nanoparticles on N-rich carbon  
1259 nanotubes via joule heating for efficient hydrogen and oxygen evolution reaction. *J.*  
1260 *Alloys Compd.* **2023**, *959*.
- 1261 63. Sun, J.-P.; Zheng, Y.; Zhang, Z.-S.; Meng, X.-C.; Li, Z.-Z., Modulation of d-orbital  
1262 to realize enriched electronic cobalt sites in cobalt sulfide for enhanced hydrogen  
1263 evolution in electrocatalytic water/seawater splitting. *Rare Metals* **2023**, *43* (2), 511-  
1264 521.
- 1265 64. Yang, C.; Yao, Y.; He, S.; Xie, H.; Hitz, E.; Hu, L., Ultrafine Silver Nanoparticles  
1266 for Seeded Lithium Deposition toward Stable Lithium Metal Anode. *Adv. Mater.* **2017**,  
1267 *29* (38).
- 1268 65. Chen, Y.; Egan, G. C.; Wan, J.; Zhu, S.; Jacob, R. J.; Zhou, W.; Dai, J.; Wang, Y.;  
1269 Danner, V. A.; Yao, Y.; Fu, K.; Wang, Y.; Bao, W.; Li, T.; Zachariah, M. R.; Hu, L.,  
1270 Ultra-fast self-assembly and stabilization of reactive nanoparticles in reduced graphene  
1271 oxide films. *Nat. Commun.* **2016**, *7* (1).
- 1272 66. Qian, F.; Peng, L.; Cao, D.; Jiang, W.; Hu, C.; Huang, J.; Zhang, X.; Luo, J.; Chen,  
1273 S.; Wu, X.; Song, L.; Chen, Q., Asymmetric active sites originate from high-entropy

- 1274 metal selenides by joule heating to boost electrocatalytic water oxidation. *Joule* **2024**,  
1275 8 (8), 2342-2356. View Article Online  
DOI: 10.1039/D4MH01180E
- 1276 67. Dou, S.; Xu, J.; Cui, X.; Liu, W.; Zhang, Z.; Deng, Y.; Hu, W.; Chen, Y., High-  
1277 temperature shock enabled nanomanufacturing for energy - related applications.  
1278 *Advanced Energy Materials* **2020**, 10 (33), 2001331-2001346.
- 1279 68. Xie, M.; Xiao, X.; Wu, D.; Zhen, C.; Wu, C.; Wang, W.; Nian, H.; Li, F.; Gu, M.  
1280 D.; Xu, Q., MOF-mediated synthesis of novel PtFeCoNiMn high-entropy nano-alloy  
1281 as bifunctional oxygen electrocatalysts for zinc-air battery. *Nano Research* **2024**, 17 (6),  
1282 5288-5297.
- 1283 69. Wang, Y.; Zhang, Y.; Xing, P.; Li, X.; Du, Q.; Fan, X.; Cai, Z.; Yin, R.; Yao, Y.;  
1284 Gan, W., Self-Encapsulation of High-Entropy Alloy Nanoparticles inside Carbonized  
1285 Wood for Highly Durable Electrocatalysis. *Adv. Mater.* **2024**, 36 (28).
- 1286 70. Dittmann, J.; Maurath, J.; Bitsch, B.; Willenbacher, N., Highly Porous Materials  
1287 with Unique Mechanical Properties from Smart Capillary Suspensions. *Adv. Mater.*  
1288 **2015**, 28 (8), 1689-1696.
- 1289 71. Wen, Z.; Tang, Z.; Liu, Y.; Zhuang, L.; Yu, H.; Chu, Y., Ultrastrong and High  
1290 Thermal Insulating Porous High-Entropy Ceramics up to 2000 °C. *Adv. Mater.* **2024**,  
1291 36 (14).
- 1292 72. Dai, X.; Liu, H.; Liu, X.; Liu, Z.; Liu, Y.; Cao, Y.; Tao, J.; Shan, Z., Silicon  
1293 nanoparticles encapsulated in multifunctional crosslinked nano-silica/carbon hybrid  
1294 matrix as a high-performance anode for Li-ion batteries. *Chem. Eng. J.* **2021**, 418.
- 1295 73. Friend, C. M.; Xu, B., Heterogeneous Catalysis: A Central Science for a  
1296 Sustainable Future. *Acc. Chem. Res.* **2017**, 50 (3), 517-521.
- 1297 74. Yuan, H.; Jiang, D.; Li, Z.; Liu, X.; Tang, Z.; Zhang, X.; Zhao, L.; Huang, M.; Liu,  
1298 H.; Song, K.; Zhou, W., Laser Synthesis of PtMo Single-Atom Alloy Electrode for  
1299 Ultralow Voltage Hydrogen Generation. *Adv. Mater.* **2023**, 36, 2305375-2305385.
- 1300 75. Shi, W.; Li, Z.; Gong, Z.; Liang, Z.; Liu, H.; Han, Y.-C.; Niu, H.; Song, B.; Chi,  
1301 X.; Zhou, J.; Wang, H.; Xia, B. Y.; Yao, Y.; Tian, Z.-Q., Transient and general synthesis  
1302 of high-density and ultrasmall nanoparticles on two-dimensional porous carbon via  
1303 coordinated carbothermal shock. *Nat. Commun.* **2023**, 14 (1).
- 1304 76. Choi, C. H. W.; Shin, J.; Eddy, L.; Granja, V.; Wyss, K. M.; Damasceno, B.; Guo,  
1305 H.; Gao, G.; Zhao, Y.; Higgs, C. F.; Han, Y.; Tour, J. M., Flash-within-flash synthesis  
1306 of gram-scale solid-state materials. *Nat. Chem.* **2024**, 1-7.
- 1307 77. Chen, W.; Cheng, Y.; Chen, J.; Bets, K. V.; Salvatierra, R. V.; Ge, C.; Li, J. T.;  
1308 Luong, D. X.; Kittrell, C.; Wang, Z.; McHugh, E. A.; Gao, G.; Deng, B.; Han, Y.;  
1309 Yakobson, B. I.; Tour, J. M., Nondestructive flash cathode recycling. *Nat. Commun.*  
1310 **2024**, 15 (1).
- 1311 78. Selvam, E.; Yu, K.; Ngu, J.; Najmi, S.; Vlachos, D. G., Recycling polyolefin plastic  
1312 waste at short contact times via rapid joule heating. *Nat. Commun.* **2024**, 15 (1).



- 1313 79. Huang, G.; Leng, Y.; Yin, Y.-C.; Das, S.; Wan, J., Perspectives on Ultrafast, Precise Synthesis and Regeneration of Advanced Battery Materials. *Energy Fuels* **2024**,  
1314 38 (15), 13722-13736.
- 1316 80. Dong, H.; Wang, L.; Cheng, Y.; Sun, H.; You, T.; Qie, J.; Li, Y.; Hua, W.; Chen,  
1317 K., Flash Joule Heating: A Promising Method for Preparing Heterostructure Catalysts  
1318 to Inhibit Polysulfide Shuttling in Li-S Batteries. *Advanced Science* **2024**.
- 1319 81. You, L.; Dong, S.; Fang, Y.; Guo, Y.; Zhu, K.; Gao, Y.; Bao, T.; Wu, H.; Cao, D.,  
1320 A graphene-like hollow sphere anode for lithium-ion batteries. *Chem. Commun.* **2024**,  
1321 60 (38), 5030-5033.
- 1322 82. Li, C.; Wang, Z.; Liu, M.; Wang, E.; Wang, B.; Xu, L.; Jiang, K.; Fan, S.; Sun, Y.;  
1323 Li, J.; Liu, K., Ultrafast self-heating synthesis of robust heterogeneous nanocarbitides for  
1324 high current density hydrogen evolution reaction. *Nat. Commun.* **2022**, 13 (1), 3338-  
1325 3349.
- 1326 83. Khan, M. A.; Al-Attas, T.; Roy, S.; Rahman, M. M.; Ghaffour, N.; Thangadurai,  
1327 V.; Larter, S.; Hu, J.; Ajayan, P. M.; Kibria, M. G., Seawater electrolysis for hydrogen  
1328 production: a solution looking for a problem? *Energy & Environmental Science* **2021**,  
1329 14 (9), 4831-4839.
- 1330 84. Zhang, Y.; Lin, Y.; Duan, T.; Song, L., Interfacial engineering of heterogeneous  
1331 catalysts for electrocatalysis. *Mater. Today* **2021**, 48, 115-134.
- 1332 85. Zhang, X.; Huang, W.; Yu, L.; García-Melchor, M.; Wang, D.; Zhi, L.; Zhang, H.,  
1333 Enabling heterogeneous catalysis to achieve carbon neutrality: Directional catalytic  
1334 conversion of CO<sub>2</sub> into carboxylic acids. *Carbon Energy* **2023**, 6 (3).
- 1335 86. Yu, Q.; Luo, Y.; Qiu, S.; Li, Q.; Cai, Z.; Zhang, Z.; Liu, J.; Sun, C.; Liu, B., Tuning  
1336 the Hydrogen Evolution Performance of Metallic 2D Tantalum Disulfide by Interfacial  
1337 Engineering. *ACS Nano* **2019**, 13 (10), 11874-11881.
- 1338 87. Xue, Z.; Li, X.; Liu, Q.; Cai, M.; Liu, K.; Liu, M.; Ke, Z.; Liu, X.; Li, G., Interfacial  
1339 Electronic Structure Modulation of NiTe Nanoarrays with NiS Nanodots Facilitates  
1340 Electrocatalytic Oxygen Evolution. *Adv. Mater.* **2019**, 31 (21).
- 1341 88. Shao, Q.; Wang, P.; Huang, X., Opportunities and Challenges of Interface  
1342 Engineering in Bimetallic Nanostructure for Enhanced Electrocatalysis. *Adv. Funct.*  
1343 *Mater.* **2018**, 29 (3).
- 1344 89. Liu, P.; Zhang, X.; Fei, J.; Shi, Y.; Zhu, J.; Zhang, D.; Zhao, L.; Wang, L.; Lai, J.,  
1345 Frank Partial Dislocations in Coplanar Ir/C Ultrathin Nanosheets Boost Hydrogen  
1346 Evolution Reaction. *Adv. Mater.* **2023**, 36 (11).
- 1347 90. Tao Meng, P. S., Feng Yang, Jie Zhu, Baoguang Mao, Lirong Zheng and Minhua  
1348 Cao, Double-atom dealloying-derived Frank partial dislocations in cobalt nanocatalysts  
1349 boost metal-air batteries and fuel cells. *Proceedings of the National Academy of*  
1350 *Sciences* **2022**, 119, e2214089119.

- 1351 91. Wulan, B.; Cao, X.; Tan, D.; Ma, J.; Zhang, J., To stabilize oxygen on In/In<sub>2</sub>O<sub>3</sub> heterostructure via joule heating for efficient electrocatalytic CO<sub>2</sub> reduction. *Adv. Funct. Mater.* **2022**, *33* (1), 2209114-2209123. View Article Online DOI: 10.1039/D4MH01180E
- 1354 92. Qiu, Y.; Hu, Z.; Li, H.; Ren, Q.; Chen, Y.; Hu, S., Hybrid electrocatalyst Ag/Co/C via flash Joule heating for oxygen reduction reaction in alkaline media. *Chem. Eng. J.* **2022**, *430*.
- 1357 93. Chen, J.; Chen, W.; Deng, B.; Li, B.; Kittrell, C.; Tour, J. M., Cathode Interface Construction by Rapid Sintering in Solid-State Batteries. *Small* **2023**, *20* (8).
- 1359 94. Yao, X.; Chen, S.; Wang, C.; Chen, T.; Li, J.; Xue, S.; Deng, Z.; Zhao, W.; Nan, B.; Zhao, Y.; Yang, K.; Song, Y.; Pan, F.; Yang, L.; Sun, X., Interface Welding via Thermal Pulse Sintering to Enable 4.6 V Solid - State Batteries. *Advanced Energy Materials* **2023**, *14* (10).
- 1363 95. Xia, D.; Mannering, J.; Huang, P.; Xu, Y.; Li, Q.; Li, H.; Qin, Y.; Kulak, A. N.; Menzel, R., Electrothermal Transformations within Graphene-Based Aerogels through High-Temperature Flash Joule Heating. *J. Am. Chem. Soc.* **2023**, *146* (1), 159-169.
- 1366 96. Yao, Y.; Huang, Z.; Xie, P.; Li, T.; Lacey, S. D.; Jiao, M.; Xie, H.; Fu, K. K.; Jacob, R. J.; Kline, D. J.; Yang, Y.; Zachariah, M. R.; Wang, C.; Shahbazian-Yassar, R.; Hu, L., Ultrafast, Controllable Synthesis of Sub-Nano Metallic Clusters through Defect Engineering. *ACS Appl. Mater. Interfaces* **2019**, *11* (33), 29773-29779.
- 1370 97. Qiao, B.; Wang, A.; Yang, X.; Allard, L. F.; Jiang, Z.; Cui, Y.; Liu, J.; Li, J.; Zhang, T., Single-atom catalysis of CO oxidation using Pt1/FeOx. *Nat. Chem.* **2011**, *3* (8), 634-641.
- 1373 98. Zhu, C.; Fu, S.; Shi, Q.; Du, D.; Lin, Y., Single-Atom Electrocatalysts. *Angew. Chem. Int. Ed.* **2017**, *56* (45), 13944-13960.
- 1375 99. Mao, J.; He, C. T.; Pei, J.; Chen, W.; He, D.; He, Y.; Zhuang, Z.; Chen, C.; Peng, Q.; Wang, D.; Li, Y., Accelerating water dissociation kinetics by isolating cobalt atoms into ruthenium lattice. *Nat. Commun.* **2018**, *9* (1), 4958-4866.
- 1378 100. Xu, G.; Liu, Q.; Yan, H., Recent Advances of Single-atom Catalysts for Electro-catalysis. *Chem. Res. Chin. Univ.* **2022**, *38* (5), 1146-1150.
- 1380 101. Guo, J.; Liu, H.; Li, D.; Wang, J.; Djitchou, X.; He, D.; Zhang, Q., A minireview on the synthesis of single atom catalysts. *RSC Advances* **2022**, *12* (15), 9373-9394.
- 1383 102. Yu, Y.; Zhu, Z.; Huang, H., Surface Engineered Single - atom Systems for Energy Conversion. *Adv. Mater.* **2024**, *36* (16).
- 1385 103. Giugni, A., Non-locality by nanoconfinement. *Nat. Nanotechnol.* **2019**, *14* (9), 814-815.
- 1387 104. Xiong, H.; Datye, A. K.; Wang, Y., Thermally Stable Single - Atom Heterogeneous Catalysts. *Adv. Mater.* **2021**, *33* (50).

- 1389 105. Yao, Y.; Huang, Z.; Xie, P.; Wu, L.; Ma, L.; Li, T.; Pang, Z.; Jiao, M.; Liang, Z.; Gao, J.; He, Y.; Kline, D. J.; Zachariah, M. R.; Wang, C.; Lu, J.; Wu, T.; Li, T.; Wang, C.; Shahbazian-Yassar, R.; Hu, L., High temperature shockwave stabilized single atoms. *Nat. Nanotechnol.* **2019**, *14* (9), 851-857.
- 1393 106. Jiang, D.; Yao, Y.; Li, T.; Wan, G.; Pereira-Hernández, X. I.; Lu, Y.; Tian, J.; Khivantsev, K.; Engelhard, M. H.; Sun, C.; García-Vargas, C. E.; Hoffman, A. S.; Bare, S. R.; Datye, A. K.; Hu, L.; Wang, Y., Tailoring the Local Environment of Platinum in Single-Atom Pt1/CeO2 Catalysts for Robust Low-Temperature CO Oxidation. *Angew. Chem. Int. Ed.* **2021**, *60* (50), 26054-26062.
- 1398 107. Zhang, J.; Wang, E.; Cui, S.; Yang, S.; Zou, X.; Gong, Y., Single-Atom Pt Anchored on Oxygen Vacancy of Monolayer Ti3C2Tx for Superior Hydrogen Evolution. *Nano Lett.* **2022**, *22* (3), 1398-1405.
- 1401 108. Wu, H.; Lu, Q.; Li, Y.; Wang, J.; Li, Y.; Jiang, R.; Zhang, J.; Zheng, X.; Han, X.; Zhao, N.; Li, J.; Deng, Y.; Hu, W., Rapid Joule-Heating Synthesis for Manufacturing High-Entropy Oxides as Efficient Electrocatalysts. *Nano Letters* **2022**, *22* (16), 6492-6500.
- 1405 109. Yu, L.; Zeng, K.; Li, C.; Lin, X.; Liu, H.; Shi, W.; Qiu, H. J.; Yuan, Y.; Yao, Y., High-entropy alloy catalysts: From bulk to nano toward highly efficient carbon and nitrogen catalysis. *Carbon Energy* **2022**, *4* (5), 731-761.
- 1408 110. Chang, R.; Li, H.; Tian, X.; Yang, Y.; Dong, T.; Wang, Z.; Lai, J.; Feng, S.; Wang, L., In Situ, Rapid Synthesis of Carbon-Loaded High Density and Ultrasmall High Entropy Oxide Nanoparticles as Efficient Electrocatalysts. *Small* **2024**, *20* (24).
- 1411 111. Yao, Y.; Dong, Q.; Brozena, A.; Luo, J.; Miao, J.; Chi, M.; Wang, C.; Kevrekidis, I. G.; Ren, Z. J.; Greeley, J.; Wang, G.; Anapolsky, A.; Hu, L., High-entropy nanoparticles: Synthesis-structure-property relationships and data-driven discovery. *Science* **2022**, *376* (6589).
- 1415 112. Yonggang Yao, Z. H., Pengfei Xie, Steven D. Lacey, Rohit Jiji Jacob, Hua Xie, Fengjuan Chen, Anmin Nie, Tiancheng Pu, Miles Rehwoldt, Daiwei Yu, Michael R. Zachariah, Chao Wang, Reza Shahbazian-Yassar, Ju Li, Liangbing Hu, Carbothermal shock synthesis of high-entropy-alloy nanoparticles. *Science* **2018**, *359*, 1489-1494.
- 1420 113. Zhang, Y.; Wang, D.; Wang, S., High-Entropy Alloys for Electrocatalysis: Design, Characterization, and Applications. *Small* **2021**, *18* (7).
- 1422 114. Rao, P.; Deng, Y.; Fan, W.; Luo, J.; Deng, P.; Li, J.; Shen, Y.; Tian, X., Movable type printing method to synthesize high-entropy single-atom catalysts. *Nature Communications* **2022**, *13* (1).
- 1425 115. Tian, X.; Li, H.; Chang, R.; Yang, Y.; Wang, Z.; Dong, T.; Lai, J.; Feng, S.; Wang, L., Rapid, self-sacrificing template synthesis of two dimensional high-entropy oxides toward high-performance oxygen evolution. *Journal of Materials Chemistry A* **2024**, *12* (6), 3276-3282.



- 1429 116. Zhao, J.; Wang, Z.; Fang, X.; Yang, L.; Wu, C.; Gan, W.; Zhou, Y.; Shan, J.; Lin, Y., Fast joule heating synthesis of NiCoFeCrMo high-entropy alloy embedded in  
1430 graphene for water oxidation. *Journal of Alloys and Compounds* **2023**, 966. View Article Online  
DOI: 10.1039/D4MH01180E
- 1432 117. Zhao, Z.; Qin, S.; Li, X.; Sun, J.; Li, Z.; Meng, X., Sulfur-facilitated in situ  
1433 deep reconstruction of transition metal molybdates toward superior electrocatalytic  
1434 oxidation of alkaline seawater. *Chem Catalysis* **2024**.
- 1435 118. Peng, H.; Ren, J.; Wang, Y.; Xiong, Y.; Wang, Q.; Li, Q.; Zhao, X.; Zhan, L.;  
1436 Zheng, L.; Tang, Y.; Lei, Y., One-stone, two birds: Alloying effect and surface defects  
1437 induced by Pt on Cu<sub>2-x</sub>Se nanowires to boost C-C bond cleavage for electrocatalytic  
1438 ethanol oxidation. *Nano Energy* **2021**, 88.
- 1439 119. Huo, S.; Song, X.; Zhao, Y.; Ni, W.; Wang, H.; Li, K., Insight into the  
1440 significant contribution of intrinsic carbon defects for the high-performance capacitive  
1441 desalination of brackish water. *Journal of Materials Chemistry A* **2020**, 8 (38), 19927-  
1442 19937.
- 1443 120. Yang, S.; Xu, S.; Tong, J.; Ding, D.; Wang, G.; Chen, R.; Jin, P.; Wang, X. C.,  
1444 Overlooked role of nitrogen dopant in carbon catalysts for peroxymonosulfate  
1445 activation: Intrinsic defects or extrinsic defects? *Applied Catalysis B: Environmental*  
1446 **2021**, 295.
- 1447 121. Li, D.; Ren, B.; Jin, Q.; Cui, H.; Wang, C., Nitrogen-doped, oxygen-  
1448 functionalized, edge- and defect-rich vertically aligned graphene for highly enhanced  
1449 oxygen evolution reaction. *Journal of Materials Chemistry A* **2018**, 6 (5), 2176-2183.
- 1450 122. Shao, P.; Yu, S.; Duan, X.; Yang, L.; Shi, H.; Ding, L.; Tian, J.; Yang, L.; Luo,  
1451 X.; Wang, S., Potential Difference Driving Electron Transfer via Defective Carbon  
1452 Nanotubes toward Selective Oxidation of Organic Micropollutants. *Environmental*  
1453 *Science & Technology* **2020**, 54 (13), 8464-8472.
- 1454 123. Gao, Y.; Liang, S.; Liu, B.; Jiang, C.; Xu, C.; Zhang, X.; Liang, P.; Elimelech,  
1455 M.; Huang, X., Subtle tuning of nanodefects actuates highly efficient electrocatalytic  
1456 oxidation. *Nature Communications* **2023**, 14 (1).
- 1457 124. Guo, L.; Chi, J.; Zhu, J.; Cui, T.; Lai, J.; Wang, L., Dual-doping NiMoO<sub>4</sub> with  
1458 multi-channel structure enable urea-assisted energy-saving H<sub>2</sub> production at large  
1459 current density in alkaline seawater. *Applied Catalysis B: Environmental* **2023**, 320.
- 1460 125. Zhou, S.; Jang, H.; Qin, Q.; Hou, L.; Kim, M. G.; Liu, S.; Liu, X.; Cho, J.,  
1461 Boosting Hydrogen Evolution Reaction by Phase Engineering and Phosphorus Doping  
1462 on Ru/P-TiO<sub>2</sub>. *Angewandte Chemie International Edition* **2022**, 61 (47).
- 1463 126. Yu, J.; Li, J.; Xu, C.-Y.; Li, Q.; Liu, Q.; Liu, J.; Chen, R.; Zhu, J.; Wang, J.,  
1464 Modulating the d-band centers by coordination environment regulation of single-atom  
1465 Ni on porous carbon fibers for overall water splitting. *Nano Energy* **2022**, 98.
- 1466 127. Ren, G.; Zhao, J.; Zhao, Z.; Li, Z.; Wang, L.; Zhang, Z.; Li, C.; Meng, X.,  
1467 Defects-Induced Single-Atom Anchoring on Metal–Organic Frameworks for High-  
1468 Efficiency Photocatalytic Nitrogen Reduction. *Angew. Chem. Int. Ed.* **2023**, 63 (2).

1469

1470

1471

128. Ren, G.; Shi, M.; Li, Z.; Zhang, Z.; Meng, X. J. A. C. B. E., Electronic metal-support interaction via defective-induced platinum modified BiOBr for photocatalytic N<sub>2</sub> fixation. **2023**, 327, 122462.

[View Article Online](#)  
[DOI: 10.1039/D4MH01180E](#)

Published on 06 November 2024. Downloaded on 11/7/2024 1:56:37 AM.

Materials Horizons Accepted Manuscript

### Data availability statements

[View Article Online](#)  
DOI: 10.1039/D4MH01180E

No primary research results, software or code have been included and no new data were generated or analysed as part of this review.